

# Global Biogeochemical Cycles®



## RESEARCH ARTICLE

10.1029/2023GB007845

### Special Section:

Regional Carbon Cycle Assessment and Processes - 2

### Key Points:

- We synthesize Australasia's carbon C-CO<sub>2</sub> budget (together with Australia and New Zealand) based on bottom-up and top-down approaches
- Australasia's bottom-up carbon budget suggests that this region was close to neutral ( $-0.4 \pm 77.0$  TgC yr<sup>-1</sup>) from 2010 to 2019
- Australasia's annual CO<sub>2</sub> balance fluctuates significantly, particularly in Australia, shifting from a strong carbon sink to a strong carbon source

### Supporting Information:

Supporting Information may be found in the online version of this article.

### Correspondence to:

Y. Villalobos,  
yohanna.villalobos@csiro.au;  
yohanna.villalobos@nateko.lu.se

### Citation:

Villalobos, Y., Canadell, J. G., Keller, E. D., Briggs, P. R., Bukosa, B., Giltrap, D. L., et al. (2023). A comprehensive assessment of anthropogenic and natural sources and sinks of Australasia's carbon budget. *Global Biogeochemical Cycles*, 37, e2023GB007845. <https://doi.org/10.1029/2023GB007845>

Received 17 MAY 2023

Accepted 6 NOV 2023

Corrected 1 JAN 2024

This article was corrected on 1 JAN 2024. See the end of the full text for details.










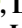


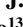





### Author Contributions:

**Conceptualization:** Yohanna Villalobos, Josep G. Canadell, Elizabeth D. Keller

© 2023. The Authors.

This is an open access article under the terms of the [Creative Commons Attribution License](#), which permits use, distribution and reproduction in any medium, provided the original work is properly cited.

## A Comprehensive Assessment of Anthropogenic and Natural Sources and Sinks of Australasia's Carbon Budget

Yohanna Villalobos<sup>1</sup> , Josep G. Canadell<sup>1</sup> , Elizabeth D. Keller<sup>2</sup> , Peter R. Briggs<sup>1</sup> , Beata Bukosa<sup>3</sup> , Donna L. Giltrap<sup>4</sup> , Ian Harman<sup>1</sup> , Timothy W. Hilton<sup>5</sup> , Miko U. F. Kirschbaum<sup>4</sup> , Ronny Lauerwald<sup>6</sup> , Liyin L. Liang<sup>4</sup>, Taylor Maavara<sup>7</sup> , Sara E. Mikaloff-Fletcher<sup>3</sup> , Peter J. Rayner<sup>8</sup> , Laure Resplandy<sup>9</sup> , Judith Rosentreter<sup>10,11</sup> , Eva-Marie Metz<sup>12</sup> , Oscar Serrano<sup>13,14</sup> , and Benjamin Smith<sup>15</sup> 

<sup>1</sup>CSIRO Environment, Canberra, ACT, Australia, <sup>2</sup>GNS Science, Lower Hutt, New Zealand and Victoria University of Wellington, Wellington, New Zealand, <sup>3</sup>NIWA, National Institute of Water and Atmospheric Research, Wellington, New Zealand, <sup>4</sup>Manaaki Whenua—Landcare Research, Palmerston North, New Zealand, <sup>5</sup>GNS Science, Lower Hutt, New Zealand, <sup>6</sup>Université Paris-Saclay, INRAE, AgroParisTech, UMR EcoSys, Palaiseau, France, <sup>7</sup>School of Geography, University of Leeds, West Yorkshire, UK, <sup>8</sup>School of Geography, Earth and Atmospheric Sciences, University of Melbourne, Melbourne, VIC, Australia, <sup>9</sup>Department of Geosciences, High Meadows Environmental Institute, Princeton University, Princeton, NJ, USA, <sup>10</sup>Faculty of Science and Engineering, Southern Cross University, Lismore, NSW, Australia, <sup>11</sup>Yale Institute for Biospheric Studies, Yale University, New Haven, CT, USA, <sup>12</sup>Institute of Environmental Physics, Heidelberg University, Heidelberg, Germany, <sup>13</sup>Centre d'Estudis Avançats de Blanes, Consejo Superior de Investigaciones Científicas, Blanes, Spain, <sup>14</sup>School of Science and Centre for Marine Ecosystems Research, Edith Cowan University, Joondalup, WA, Australia, <sup>15</sup>Hawkesbury Institute for the Environment, Western Sydney University, Richmond, NSW, Australia

**Abstract** Regional carbon budget assessments attribute and track changes in carbon sources and sinks and support the development and monitoring the efficacy of climate policies. We present a comprehensive assessment of the natural and anthropogenic carbon (C-CO<sub>2</sub>) fluxes for Australasia as a whole, as well as for Australia and New Zealand individually, for the period from 2010 to 2019, using two approaches: bottom-up methods that integrate flux estimates from land-surface models, data-driven models, and inventory estimates; and top-down atmospheric inversions based on satellite and in situ measurements. Our bottom-up decadal assessment suggests that Australasia's net carbon balance was close to carbon neutral ( $-0.4 \pm 77.0$  TgC yr<sup>-1</sup>). However, substantial uncertainties remain in this estimate, primarily driven by the large spread between our regional terrestrial biosphere simulations and predictions from global ecosystem models. Within Australasia, Australia was a net source of  $38.2 \pm 75.8$  TgC yr<sup>-1</sup>, and New Zealand was a net CO<sub>2</sub> sink of  $-38.6 \pm 13.4$  TgC yr<sup>-1</sup>. The top-down approach using atmospheric CO<sub>2</sub> inversions indicates that fluxes derived from the latest satellite retrievals are consistent within the range of uncertainties with Australia's bottom-up budget. For New Zealand, the best agreement was found with a national scale flux inversion estimate based on in situ measurements, which provide better constrained of fluxes than satellite flux inversions. This study marks an important step toward a more comprehensive understanding of the net CO<sub>2</sub> balance in both countries, facilitating the improvement of carbon accounting approaches and strategies to reduce emissions.

**Plain Language Summary** Human activities—including the extraction and use of fossil fuels (coal, oil, and natural gas), cement production, and land-use change (e.g., land clearing), release carbon dioxide (CO<sub>2</sub>) to the atmosphere, while biospheric processes such as the CO<sub>2</sub> uptake by forests and revegetation remove CO<sub>2</sub> from the atmosphere. In this study, we assess the balance of natural and human-driven sources and sinks of CO<sub>2</sub> for Australia and New Zealand (referred to as the Australasia carbon budget) for 2010–2019. Our findings indicate that Australasia was close to carbon neutral, with large uncertainties, suggesting that the CO<sub>2</sub> sinks from vegetation in this region largely offset the CO<sub>2</sub> emissions from human activities. An independent assessment using the latest satellite observations and modeling shows consistent results for Australia. For New Zealand, a national system of ground observations and modeling agreed better with the bottom-up budget than satellite-derived flux estimates.

## 1. Introduction

Carbon budgets are comprehensive assessments of anthropogenic and natural sources and sinks of carbon, providing key information for the development of international and national climate policies (Canadell, Costa,

**Data curation:** Peter R. Briggs, Beata Bukosa, Donna L. Giltrap, Timothy W. Hilton, Ronny Lauerwald, Liyin L. Liang, Taylor Maavara, Laure Resplandy, Judith Rosentreter, Eva-Marie Metz

**Formal analysis:** Yohanna Villalobos, Josep G. Canadell, Elizabeth D. Keller, Beata Bukosa, Donna L. Giltrap, Ian Harman, Miko U. F. Kirschbaum, Judith Rosentreter

**Investigation:** Yohanna Villalobos, Elizabeth D. Keller, Beata Bukosa, Miko U. F. Kirschbaum, Ronny Lauerwald, Taylor Maavara, Sara E. Mikaloff-Fletcher, Peter J. Rayner, Laure Resplandy, Judith Rosentreter, Eva-Marie Metz, Oscar Serrano, Benjamin Smith

**Methodology:** Josep G. Canadell, Elizabeth D. Keller, Ian Harman

**Software:** Elizabeth D. Keller, Beata Bukosa, Donna L. Giltrap

**Supervision:** Josep G. Canadell

**Visualization:** Yohanna Villalobos

**Writing – original draft:** Yohanna Villalobos, Josep G. Canadell, Elizabeth D. Keller

**Writing – review & editing:** Yohanna Villalobos, Josep G. Canadell, Elizabeth D. Keller, Peter R. Briggs, Beata Bukosa, Donna L. Giltrap, Ian Harman, Timothy W. Hilton, Miko U. F. Kirschbaum, Ronny Lauerwald, Taylor Maavara, Sara E. Mikaloff-Fletcher, Judith Rosentreter, Eva-Marie Metz, Benjamin Smith

et al., 2021; Canadell, Meyer, et al., 2021; Friedlingstein et al., 2022; Matthews et al., 2020). With this purpose, the second phase of the REgional Carbon Cycle Assessment and Processes (RECCAP-2) (Ciais et al., 2022) coordinated by the Global Carbon Project (GCP), has developed regional CO<sub>2</sub>, methane (CH<sub>4</sub>), and nitrous oxide (N<sub>2</sub>O) budgets for the entire globe, covering 10 land regions (North America, South America, Europe, Africa, West Asia, South Asia, East Asia, Russia, Southeast Asia, and Australasia), five ocean basins (Pacific Ocean, Atlantic Ocean, Southern Ocean, Arctic Ocean, and Indian Ocean), and two regions of special interest (permafrost and polar regions) (Poulter et al., 2022).

RECCAP-2 budgets are different from the national GHG inventories (NGHGs) prepared by governments and submitted to the United Nations Framework Convention on Climate Change (UNFCCC). NGHGs provide country-level emission estimates from human activities based on sector activity data or by targeting all GHG fluxes for the same sectors in areas defined as managed lands (Grassi et al., 2023). RECCAP-2 budgets cover all lands of a region (managed and unmanaged) and include all natural and anthropogenic sources and sinks estimated with process-based land-surface models, atmospheric information and modeling, and a myriad of independent data sources and estimates that also includes data from the NGHGs.

In this study, we build a carbon budget for one of the RECCAP-2 land regions, Australasia, which consists of Australia and New Zealand. For the first phase of RECCAP (RECCAP-1), a carbon budget for Australia was produced for the period 1990–2011 (Haverd et al., 2013). Other studies have addressed components of the role and dynamics of Australia and New Zealand's biospheric fluxes (Baisden et al., 2001; Beringer et al., 2022; Haverd et al., 2016; Roxburgh et al., 2004; Tate et al., 2000; Teckentrup et al., 2021; Trotter et al., 2004; Trudinger et al., 2016; Wang & Barrett, 2003). In addition, recent studies have provided estimates of the net carbon balance of these countries based on global and regional atmospheric inversions (Byrne et al., 2023; Steinkamp et al., 2017; Villalobos et al., 2022). The reconciliation between bottom-up and top-down approaches remains a challenge because bottom-up approaches often report only a sub-set of all fluxes, while atmospheric inversions have their own limitations, such as having few surface observations and low resolution of satellite products.

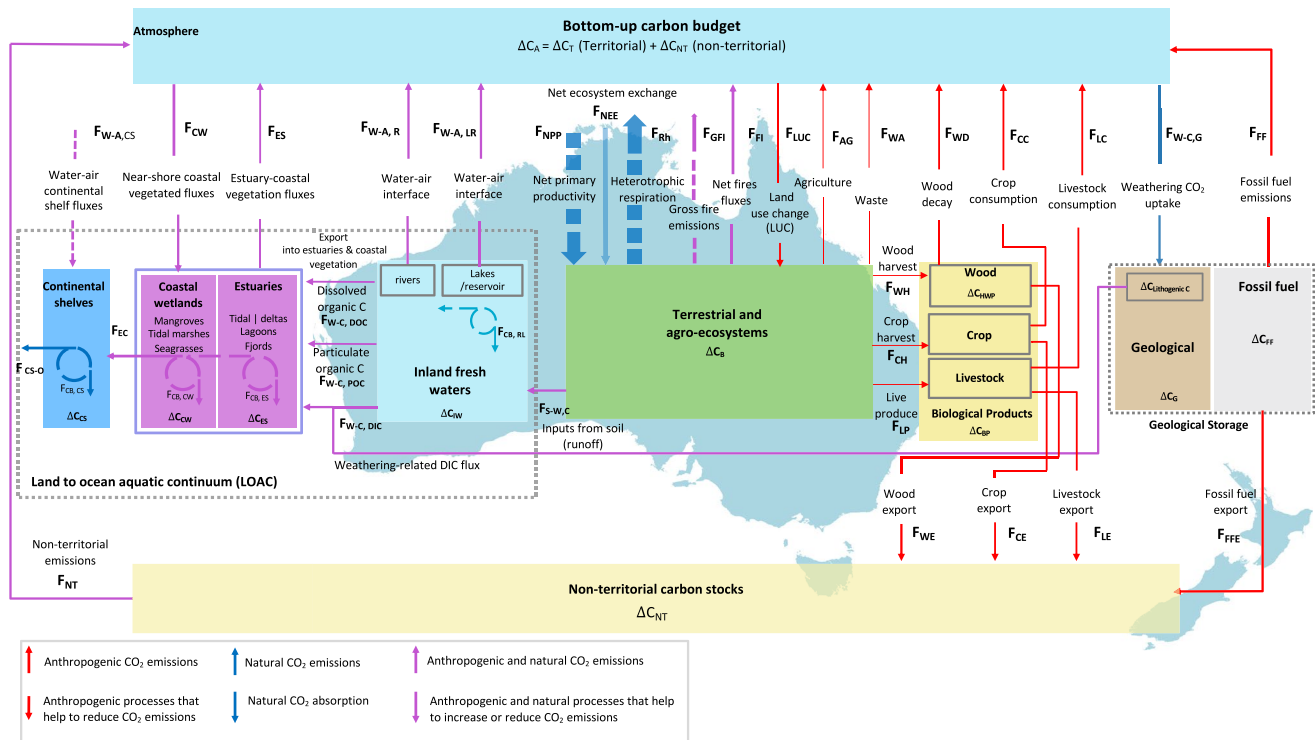
Here, we greatly expand previous work by providing for the first time a territorial carbon budget assessment that incorporates (a) all major natural and anthropogenic carbon fluxes; (b) the complete components of the land-to-ocean aquatic continuum (LOAC) system (i.e., carbon fluxes from river and lakes, reservoirs, estuaries, mangroves, salt marshes, and seagrasses, and continental shelves); and (c) an assessment of the net CO<sub>2</sub> balance for Australia and New Zealand based on global and regional inverse CO<sub>2</sub>-flux estimates, which rely on satellite-based CO<sub>2</sub> remote sensing and in situ measurements.

In addition to the territorial carbon budget quantified using the bottom-up and top-down approaches, we estimated non-territorial emissions, which are the emissions associated with the net trade of fossil fuels, crop, wood, and livestock to and from other countries. Non-territorial emissions from these products occur in the country where they are consumed, and not in Australasia where they are extracted or produced and subsequently exported outside the country. These emissions are not considered under the UNFCCC reporting guidelines, which require countries to report on their territorial anthropogenic emissions only. However, non-territorial emission estimates provide insights into the territorial origins of carbon emitted elsewhere and support exploring additional climate policy options to reduce global anthropogenic emissions.

We structure this paper as follows: Section 1, this introduction. Section 2 describes the methods of the bottom-up and top-down approaches used in this study. Section 3 provides a synthesis of results for the bottom-up carbon budget for Australasia, and for Australia and New Zealand separately, for 2010–2019, and the results of different CO<sub>2</sub> atmospheric inversions (top-down approaches). Section 4 discusses the results and attempts to reconcile the different approaches and estimates. Supporting Information S1 provides a detailed description of the methods and data used to estimate each individual flux component of the budgets, and additional results.

## 2. Methods

We followed the RECCAP-2 land carbon definition methods published by Ciais et al. (2022) to provide a full assessment of the carbon balance for Australasia (Figure 1). We note that for the construction of the budget, we did not account for carbon embedded in CH<sub>4</sub>, carbon monoxide (CO), or volatile organic compound (VOC) fluxes, and the carbon estimates provided in this study are based on the land–atmospheric CO<sub>2</sub> exchange (in and out) of the carbon pools (vertical arrows in Figure 1) and the lateral solid carbon transfer from these pools to the ocean



**Figure 1.** Diagram representing the major components of the Australasia carbon budget (bottom-up approach). Carbon stocks are shown in and out of the atmosphere as vertical solid arrows, and lateral transfers as horizontal solid arrows. Fluxes with dashed arrows are not part of either  $\Delta C_T$  or  $\Delta C_{NT}$  but are shown in the diagram because they represent important information about the carbon cycle of the region.

and trade overseas (horizontal arrows in Figure 1). We defined the territory atmospheric net carbon balance ( $\Delta C_T$ , Section 2.1) as the net carbon flux of all territorial anthropogenic and natural carbon sources and sinks to and from the atmosphere. In addition, we also estimated the non-territorial emissions ( $\Delta C_{NT}$ ).  $\Delta C_T$  and  $\Delta C_{NT}$ , together (Equation 1), represent the total net impact of territorial and non-territorial emissions ( $\Delta C_A$ ) on atmospheric  $CO_2$ ,

$$\Delta C_A = \Delta C_T + \Delta C_{NT} \quad (1)$$

Here,  $\Delta C_T$  was estimated using bottom-up (Section 2.1) and top-down approaches (Section 2.2), while  $C_{NT}$  was calculated using bottom-up methods. We describe both approaches in the section below.

## 2.1. Bottom-Up Approach

### 2.1.1. Territorial Atmospheric Net Carbon Balance

We estimated  $\Delta C_T$  (Equation 2) as the sum of all vertical carbon fluxes ( $F$ ) that flow in and out of the terrestrial ( $\Delta C_B$ ), biological product ( $\Delta C_{BP}$ ), geological ( $\Delta C_G$ ), and fossil fuel pools ( $\Delta C_{FF}$ ), as well as the individual pools of the land-to-ocean aquatic continuum (LOAC): inland water ecosystem ( $\Delta C_{IW}$ ), estuaries ( $\Delta C_{ES}$ ) and coastal wetlands ( $\Delta C_{CW}$ ) (Figure 1). Fluxes from the continental shelves ( $F_{W-A,CS}$ ) were not included in the budgets or net carbon balance of Australasia.

$$\Delta C_T = (-F_{NEE} + F_{FI} - F_{LUC} + F_{AG} - F_{WA}) + (F_{W-A,R} + F_{W-A,LR}) + (F_{ES} - F_{CW}) + (F_{WD} + F_{CC} + F_{LC}) + F_{WA} + F_{FF} \quad (2)$$

We adopt the atmospheric and climate viewpoints to determine the sign of fluxes. A negative sign in vertical fluxes ( $F$ ) indicates a removal from the atmosphere (a sink to the land), and a positive value indicates an addition to the atmosphere (a source from the land, freshwaters, and estuaries). However, a positive sign of the net carbon stock change,  $\Delta C$ , indicates an increased carbon stock in the atmosphere, land, or freshwater pools. Consistent with this definition, ecosystem productivity quantities such as gross primary productivity (GPP) or net primary

production (NPP) have positive signs. In this section, we briefly explain the bottom-up components. A summary of the data product and references/uncertainties are described in Table 1 and the Supporting Information S1.

Dominant vertical carbon fluxes in  $\Delta C_B$ , such as primary productivity ( $F_{NPP}$ ) and heterotrophic respiration ( $F_{RH}$ ), and net ecosystem productivity ( $F_{NEP}$ ; referred to as  $F_{NEE}$  in Figure 1) were calculated by combining three different model simulations: CABLE-POP model for Australia (Text S1.1 in Supporting Information S1), the Biome-BGCMuso and CenW models for New Zealand (Text S1.3 in Supporting Information S1). Each of the models was driven by their own regional drivers and observations, which leads to better and more realistic quantification of the land fluxes than global simulations.

CABLE-POP simulations for Australia were run from 1900 to 2019 under two simulation cases. For the first case (defined as scenario S2), the CABLE model was only driven by changes in climate and rising atmospheric  $CO_2$  concentration, while in the second scenario (S3), the model also included the effect of land use change in addition to changes in  $CO_2$  concentration and climate. For case S3, CABLE-POP uses the Land-Use Harmonization data set (LUH2). However, for the last 10 years of simulation, we replaced the LUH2 LUC flux with the Australian NGHGI LUC flux (referred to as  $F_{LUC}$  in Figure 1). We did this because  $F_{LUC}$  fluxes derived from the LUH2 global data set vastly differ from the nationally based and high-resolution estimates used in the Australian NGHGI reports (Text S1.1, Figures S16 and S17 in Supporting Information S1).  $F_{NPP}$ ,  $F_{RH}$ , and  $F_{NEP}$  simulated by CABLE-POP were also adjusted by the land use change effect (S3-S2). Further note that both Australia and New Zealand consider all lands to be managed lands for the purposes of the NGHGI, with relatively small exceptions to both countries. For Australia, 93% of the total land is managed, and for New Zealand, only wetlands are considered unmanaged.

To assess the carbon flux uncertainties ( $F_{NPP}$ ,  $F_{GPP}$ ,  $F_{NEE}$ ) for both Australia and New Zealand simulations, we computed the multi-model ensemble spread (standard deviation) between our regional predictions and simulations from a suite of different global ecosystem models (i.e., TRENDY simulations obtained from the GCP Global Carbon Budget; Friedlingstein et al., 2020) (Text S1.1.3 in Supporting Information S1). Here, the uncertainties do not represent errors within the model per se but rather a static analysis between our regional estimate and the current knowledge of different global ecosystem simulations. Model uncertainties associated with parameter values or driving forcing (such as meteorological data) must be carefully quantified; however, that work is beyond the scope of this study.

New Zealand's NGHGI land sector does not report net fire emissions, which is negligible in comparison with Australia, and these are accounted indirectly within New Zealand's  $F_{LUC}$  estimate (Figure 3). For Australia, the net carbon emissions from fires ( $F_{FI}$ ), i.e., fire emission counterbalanced by the  $CO_2$  uptake during post-fire vegetation recovery (Text S3.1 in Supporting Information S1), were obtained from the Australian NGHGI report. Here, the contribution of  $F_{FI}$  was restricted to temperate forests and tropical savanna ecosystems, as we assume that the rest of Australia dominated by herbaceous ecosystems, the balance of gross fire emissions and post-fire sequestration is carbon neutral (Figure S1 in Supporting Information S1). In addition, we also provide the net gross fire fluxes for Australia and New Zealand derived from global fire data sets: GFED, GFAS, and QFED (Text S3.2 in Supporting Information S1). Uncertainties from  $F_{LUC}$ ,  $F_{FI}$  and  $\Delta C_{HWP}$  correspond to the uncertainties reported in the NGHGI land sector. Uncertainties reported in the agricultural ( $F_{AG}$ ), and waste ( $F_{WA}$ ) components were also taken from the NGHGI report (Text S5 in Supporting Information S1). Carbon fluxes from the fossil fuel emissions were also obtained from Australia and New Zealand NGHGI reports. However, because these reports only provide information under energy and industry sectors, the attribution of emissions to coal, oil, gas, and cement production ( $F_{FF}$ ) (Text S4 in Supporting Information S1) was obtained from Andrew and Peters (2021), which uses the NGHGIs as primary data sources. We assigned a 5% uncertainty to  $F_{FF}$  emissions, consistent with the high confidence given to most fossil fuel emissions derived from IEA statistics and the Global Carbon Project.

Some lateral carbon fluxes in  $\Delta C_B$ , such as the carbon transport from soils to inland water  $F_{S-W,C}$  (i.e., carbon leached or eroded from soils) were estimated by mass balance (Equation 3). In Equation 3, we considered fluxes from river ( $F_{RI}$ ) (Text S6.1.1 in Supporting Information S1), lakes/reservoirs outgassing ( $F_{LR}$ ) (Text S6.1.4 in Supporting Information S1), and the lateral transfer of dissolved organic carbon (DOC) ( $F_{W-C,DOC}$ ) and particulate organic carbon (POC) ( $F_{W-C,POC}$ ) (Text S6.1.3 in Supporting Information S1) that goes into estuaries and coastal wetlands, and the carbon burial rates in lakes and reservoirs (Text S6.1.5 in Supporting Information S1). River transfers of DIC sourced from chemical rock weathering (geological carbon pool) were also included in this estimate. While inland water uncertainties from both  $F_{RI}$  and  $F_{LR}$  were calculated based on different peer-reviewed published studies (as reviewed in Lauerwald et al. (2023); Table S1 in Supporting Information S1), uncertainties from lateral carbon transport such as DOC, POC, and DIC were assumed to be a relative uncertainty of 50% as described in Ciaia et al. (2021).



**Table 1**  
A Summary of the Description/References of the Bottom-Up and Top-Down Components Used for the Carbon Budget Assessment

Method	Australia	New Zealand	SI
Bottom-up	Source/uncertainty reference	Source/uncertainty reference	Text S1.1 in Supporting Information S1 Text S1.3 in Supporting Information S1
$F_{NPP}$ , $F_{Rh}$ , $F_{NPP} - F_{Rh}$ in the absence of fire and LUC).	An updated version of CABLE-POP model (Haverd et al., 2018). (S3-S2) Simulations S2 ( $CO_2 + climate$ ), S3 ( $CO_2 + climate + LUC$ ). Uncertainties were defined as the standard deviation between CABLE-POP BIOS3 and 13 DGVM models (CABLE POP, CLASSIC, CLM5.0, IBIS, ISBA-CTRIP, JSBACH, LPJ-GUESS, LPJ, LPX-Bern, OCN, ORCHIDEE, VISIT, and YIBs).	Biome BGCMuso (Hidy et al., 2016, 2022), CenW model (Kirschbaum, 1999). Uncertainties represent the standard deviation between Biome BGCMuso/CenW and 16 global DGVM models (CABLE POP, CLASSIC, CLM5.0, DLEM, IBIS, ISAM, ISBA-CTRIP, JSBACH, LPJ-GUESS, LPJ, LPX-Bern, OCN, ORCHIDEE, SDGVM, VISIT, and YIBs).	
$F_{NPP}$ , $F_{Rh}$	Both flux components were simulated by CABLE-POP (S3 run), adjusted by LUC. $F_{Rh}$ corrected by lateral carbon export. Uncertainties were defined as the standard deviation between CABLE-POP BIOS3 and 14 DGVM models	Biome BGCMuso (Hidy et al., 2016, 2022), CenW model (Kirschbaum, 1999) Standard deviation between Biome BGCMuso/CenW and 15 DGVM models	Text S1.1 in Supporting Information S1 Text S1.3 in Supporting Information S1
$F_{LUC}$	Land use fluxes and its uncertainties were obtained from the Australia's NGHGI report. $F_{LUC}$ exclude net fire fluxes ( $F_{FI}$ ) and harvested wood products (HWPs)	New Zealand's National Greenhouse inventory (New Zealand Ministry for the Environment, 2021)	Text S2.1 in Supporting Information S1 Text S2.2 in Supporting Information S1
$F_{FI}$	Net fire emissions (fire emissions balanced by vegetation regrowth), and uncertainties were obtained from the Australia's NGHGI report	New Zealand' National GHG Inventory does not explicitly report fire emission; however, fire contribution is embedded in $F_{LUC}$ . We note fires emissions are negligible in New Zealand	Text S3.1 in Supporting Information S1
$F_{GFI}$	Ensemble mean between GFED4.s (van der Werf et al., 2017), QFED (Darrenov and da Silva, 2015), GFAS (Kaiser et al., 2012). Uncertainties represent the ensemble spread (standard deviation) between GFED, QFED, and GFAS	Same approach as in Australia	Text S3.2 in Supporting Information S1
$F_{AG}$	Australia National GHG Inventory report (Australian National Inventory Report, 2019). Uncertainties describe in the Australia's NGHGI report	New Zealand' National GHG Inventory report (New Zealand Ministry for the Environment, 2021). Uncertainties describe in the New Zealand NGHGI report	Text S5 in Supporting Information S1
$F_W$	Australia's NGHGI (Australian National Inventory Report, 2019) Uncertainties are described in the National inventory report	New Zealand's NGHGI (New Zealand Ministry for the Environment, 2021). Uncertainties are described in the National inventory report	Text S5 in Supporting Information S1
$F_{WHI}$ , $F_{WD}$ , $F_{WFI}$ , $F_{WCH}$ , $F_{CC}$ , $F_{CE}$ , $F_{LP}$ , $F_{LC}$ , $F_{LE}$	Emissions due to harvested wood products (HWPs), crop, and livestock products were calculated following Peters et al. (2012) approach. We assumed an uncertainty of 30% for wood consumption, and 20%, and 25% for crops and livestock (Ciais et al., 2021; Haverd et al., 2013)	Same approach as in Australia	Text S7 in Supporting Information S1
$F_{FF}$	Fossil fuel emissions (Andrew & Peters, 2021). Uncertainties were assumed to be 5% of the mean flux estimate	Same approach as in Australia	Text S4 in Supporting Information S1
$F_{FFE}$	Calculated consistent with the IPCC tier 2 approach, using country-specific emission factors. Uncertainties were assumed to be 5% of the mean flux estimate	Calculated consistent with the IPCC tier 2 approach, using country-specific emission factors. Uncertainties were assumed to be 5% of the mean flux estimate	Text S4 in Supporting Information S1

**Table 1**  
*Continued*

Method	Australia	New Zealand
Bottom-up	Source/uncertainty reference	Source/uncertainty reference
$F_{WA}$	Weathering CO <sub>2</sub> carbon uptake (Hartmann et al., 2009 with corrections for temperature and soil shielding from Hartmann et al., 2014). Uncertainties were assumed to be 50% of the mean flux estimate (Ciais et al., 2021)	Same approach as in Australia
$F_{W-A,R}$ ; $F_{W-A,L,R}$	River and lake water CO <sub>2</sub> evasion. Data from peer-reviewed publications rescaled to Australia (Lauerwald et al., 2023). Uncertainties were calculated as the ensemble spread (standard deviation) between these different peer-reviewed rescaled publications	Text S6.1.1 in Supporting Information S1 Text S6.1.4 in Supporting Information S1
$F_{W-C,DIC}$	Weathering related DIC flux (Hartmann et al., 2009 with correction for temperature and soil shielding effects after Hartmann et al., 2014). Uncertainties were assumed to be 50% of the mean flux estimate	Text S6.1.2 in Supporting Information S1
$F_{W-C,DOC}$ ; $F_{W-C,POC}$	Lateral carbon fluxes (DOC and POC) (Mayorga et al., 2010). Uncertainties were assumed to be 50% of the mean flux estimate (Ciais et al., 2021)	Text S6.1.3 in Supporting Information S1
$F_{CB,RL}$	Organic carbon (OC) burial in lakes and reservoir was calculated using four different global OC burial rate estimates made within the geographical zones of COSCAT (Maavara et al., 2017; Mendonça et al., 2017). Uncertainties represent the standard deviation between these 4 estimates	Text S6.1.5 in Supporting Information S1
$F_{ES}$	Data-driven (water-air CO <sub>2</sub> based on data from peer-reviewed publications (Rosentreter et al., 2023). Full statistics from a non-parametric bootstrapping approach	Text S6.2.1 in Supporting Information S1
$F_{CW}$	Data-driven method-upscaling of eddy-covariance data (Rosentreter et al., 2023). Full statistics from a non-parametric bootstrapping approach	Text S6.2.3 in Supporting Information S1
$F_{CB,ES}$	Combined routing from Maavara et al., 2019 for estuaries with OC burial equations modeled in Maavara et al. (2017)	Text S6.2.2 in Supporting Information S1
$F_{CB,CW}$	Soil carbon sequestration rates in coastal wetlands (Serrano et al., 2019)	-
$F_{CB,CW}$	Air-sea CO <sub>2</sub> fluxes in continental shelves were calculated as the average between the ensemble mean of 4 observational pCO <sub>2</sub> -based products (CarboScope, CMEMS, Coastal-SOM-FFN, Merged-SOM-FFN) and 11 ocean-based-process models (CESM-CCSM, CNRM 0.25, CNRM 1, FESOM, FESOM-BOLD, IPSL-PICES, MOM6, MRI-ESM2, MPI-HAMOC, NEMO-PlankTOM5, NorESM) (Resplandy et al., 2023). Uncertainties were calculated as the absolute difference between the mean of pCO <sub>2</sub> product and models.	Text 6.3 in Supporting Information S1

**Table 1**  
Continued

Top-down	Source/uncertainty reference	SI
Regional inversion	CMAQ OCO-2 inversion (Villalobos et al., 2022). Uncertainties (OSSEs experiments; Villalobos et al., 2020)	New Zealand's national scale inverse modeling system (part of the CarbonWatch-NZ research program, (Bukosa et al., 2023; Steinkamp et al., 2017)
Global Inversions	Five GCP global inversions (Friedlingstein et al., 2020); MIROC4-ACTM (ensemble mean and spread of 16 sets of inversion; Chandra et al., 2022); OCO-2 MIP (ensemble mean and spread of 12 global inversions; Byrne et al., 2023); GOSAT TM5-4DVAR (mean and uncertainties as the absolute difference between ACOS and RemoTeC inversions; Metz et al., 2023)	Same approach as in Australia

$$F_{S-W,C} = F_{W-A,R} + F_{W-A,L,R} + F_{W-C,DOC} + F_{W-C,POC} + F_{W-C,DIC} + F_{CB-RL} \quad (3)$$

Other lateral carbon fluxes in  $\Delta C_B$  are related to the production of crop and wood for human and animal consumption. Here, these lateral fluxes were defined as  $F_{HW}$  (harvested wood production flux) and  $F_{CH}$  (crop production flux) (Text S7 in Supporting Information S1). We only considered the carbon pool in harvested wood products ( $\Delta C_{HWP}$ ), and changes in other product pools were considered negligible on annual to decadal scales. Uncertainties around  $\Delta C_{HWP}$  correspond to the uncertainties described in the NGHGI.

Carbon loss due to decay (or decomposition) of wood products ( $F_{WD}$ ) was calculated by mass balance (Equation 4), which considers the gross production of wood harvest, wood export and import, and what is storage in  $\Delta C_{HWP}$  as follows:

$$F_{WD} = F_{WH} - (\Delta C_{HWP} + F_{WE}) + F_{IMP} \quad (4)$$

Given that  $F_{Rh}$  was simulated by land surface process models (Texts S1.1 and S1.3 in Supporting Information S1), which do not represent the influences of harvesting wood or crop, or the carbon that is transported from soils to inland waters,  $F_{Rh}$  was adjusted for these influences. We subtracted the effect of harvest ( $F_{WH}$ ,  $F_{CH}$ ,  $F_{LP}$ ), and  $F_{S-W,C}$  from  $F_{Rh}$ , because once the crops or wood are harvested and exported elsewhere, it cannot be respired by plants.

We also considered the weathering-related dissolved inorganic carbon (DIC) flux (Text S6.1.2 in Supporting Information S1) transported into estuaries and coastal wetlands. This carbon flux is sourced to a large part from  $CO_2$  that is sequestered in the weathering process and to a smaller part from the dissolution of carbonate minerals. They represent an important source of dissolved carbon that goes to rivers, estuaries, and coastal wetlands.

Air-water  $CO_2$  exchange in estuaries (Text S6.2.1 in Supporting Information S1) and coastal wetlands (Text S6.2.3 in Supporting Information S1) were represented as  $F_{ES}$  and  $F_{CW}$ , respectively.  $F_{CW}$  represents the  $CO_2$  net ecosystem exchange (NEE) in the near-shore coastal vegetation ecosystems (mangrove forests, salt marshes, and submerged seagrass meadows) with salinity  $>0.5$ . Here, NEE also uses the atmospheric convention; therefore, a negative sign denotes carbon uptake by the ecosystem and a positive NEE denotes  $CO_2$  release into the atmosphere. These estimates rely on a global upscaling method based on global averages taken from eddy-covariance measurements across other regions in the world (Rosentreter et al., 2023). Freshwater tidal marshes ( $<0.5$  salinity) were excluded as well as unvegetated coastal areas such as sandy sediments and bare rocks. Estuaries and coastal wetland uncertainties were derived from bootstrapping methods where a full set of statistics including the first (Q1) and third (Q3) quartiles of the data sets were generated (see uncertainty analysis section in Rosentreter et al., 2023). From this full set of statistics, we calculated the associate standard deviation included in this study. We also included the soil carbon rates of coastal wetlands for Australia (Serrano et al., 2019) and estuaries (Section S6.2.2 in Supporting Information S1) represented by  $F_{CB,CW}$ ,  $F_{CB,ES}$ , respectively.

We also provide the fluxes from the continental shelves ( $F_{W-A,CS}$ ) (Text S6.3 in Supporting Information S1); however, we did not incorporate these fluxes in the Australasia land budget (vertical dash arrow in Figure 1).  $F_{EC}$  represent the lateral carbon flux transferred from estuaries and coastal wetland systems to continental shelves and  $F_{CS,O}$  is the lateral carbon export from continental shelf water to the open ocean. Continental shelf waters (the shallow part of the ocean down to shelf break) were defined by Laruelle et al. (2017) where the seaward boundary is 300 km (about 186.41 mi) from shore or the 1,000-m isobath. Uncertainties associated with shelf fluxes were calculated as the absolute difference between the mean of 4  $pCO_2$ -based products, and 11 ocean based-process models (Resplandy et al., 2023) as described in Text S6.3 in Supporting Information S1.

### 2.1.2. Non-Territorial Carbon Emissions

Non-territorial emissions ( $\Delta C_{NT}$ ) are  $CO_2$  emissions from the consumption of fossil fuel ( $FF_{FE}$ ), wood ( $F_{EW}$ ), crop ( $F_{CE}$ ) and livestock ( $F_{LE}$ ) extracted or produced in Australasia but consumed overseas (Equation 5). We base our estimates on data sets from the FAOSTAT data platform (Text S7 in Supporting Information S1).

$$F_{NT} = F_{WE} + F_{CE} + F_{LE} + F_{FFE} \quad (5)$$

## 2.2. Top-Down Approach: Net Carbon Flux Balance Derived From Inverse Modeling

To build confidence in the robustness of the Australian and New Zealand bottom-up budgets, we also evaluated the net carbon balance of those two countries using global and regional atmospheric inversion frameworks (top-down approaches). For this assessment, we selected global and regional inversion-based flux estimates. Global from the Global Carbon Project (GCP) (Friedlingstein et al., 2020), MIROC4-ACTM (Chandra et al., 2022), OCO-2 MIP (Byrne et al., 2023), and GOSAT TM5-4DVAR (Metz et al., 2023). Regional from two independent inversion systems, one developed in Australia (Villalobos et al., 2022) and the other in New Zealand (Bukosa et al., 2023; Steinkamp et al., 2017). All these inversions follow the same Bayesian inversion principles, where the goal is to find an optimal estimate of CO<sub>2</sub> surface fluxes that fits both observations and a prior (or background) weighted by their uncertainties (Ciais et al., 2010; Rayner, 2020).

From the GCP global carbon budget, we calculated the ensemble mean of five different global inversion-based flux estimates (CAM5, Jena Carbon Scope, CTE, University of Edinburgh (UoE), and CMS-flux). Prior fluxes (i.e., biosphere, fires, ocean, and fossil fuel emissions) as well as atmospheric observations are described in the references provided in Table A4 in Friedlingstein et al. (2020). The inverted fluxes selected from the GCP and MIROC4-ACTM rely on only in situ observations (i.e., GLOBALVIEW-CO<sub>2</sub>, NRT or WDCGG data products). See Table 1 for a description of the MIROC4-ACTM inversion set up (Chandra et al., 2022).

From Byrne et al. (2023), we obtained the ensemble CO<sub>2</sub> flux derived from 12 independent global atmospheric inversions (OCO-2 MIP) using version 10 of NASA's ACOS full-physics retrieval algorithm (Table 1 in Byrne et al., 2023): AMES, PCTM, CAM5, CMS-Flux, CSU, CT, OU, TM5-4DVAR, UT, COLA, and WOMBAT. We selected two different flux estimates from OCO-2 MIP: (a) inversions that assimilate only OCO-2 satellite data and (b) inversions that assimilate OCO-2 satellite in combination with in situ measurements. Further to this assessment, we also included the ensemble mean of OCO-2 MIP based on previous ACOS retrieval (version 9) (Peiro et al., 2022).

We calculated two GOSAT flux estimates derived from the TM5-4DVAR inversion (Metz et al., 2023). One flux was derived from two independent GOSAT retrievals (ACOS and RemoTeC), and another derived from GOSAT (ACOS and RemoTeC) but combined with in situ measurements.

OCO-2 CMAQ regional CO<sub>2</sub> flux estimate was selected from Villalobos et al. (2022). This regional inverse system was set up to estimate fluxes across the Australian domain, including the New Zealand region, for 2015–2019. This regional inverse system was configured to assimilate OCO-2 satellite data using version 9 of NASA's ACOS retrieval algorithm. Prior biosphere information in this system relies on regional CABLE-POP model simulations, with other fluxes (i.e., fossil fuel, ocean) derived from global products ODIAC (version 2019; Oda et al., 2018), and EDGAR (version 5; Crippa et al., 2020) and CAM5 v19r1 inversion product produced by the European Center for Medium-Range Weather Forecasts (ECMWF).

Regional inversion-based fluxes from New Zealand were selected from a national inverse system developed in this country under a 5-year research program called CarbonWatch-NZ. Here, we used new estimates of this inversion system (Bukosa et al., 2023) set up for the 2011–2019 period. For this national inversion, prior biosphere fluxes were obtained from the same models as the one used to build New Zealand's bottom-up budget, which combines information derived from Biome-BGCMuSo and CenW simulation (Text S8.1 in Supporting Information S1). For this study, the inversion system was set up to assimilate in situ information obtained from two monitoring stations: Baring Head and Lauder (Brailsford et al., 2012; Lowe et al., 1979; Steinkamp et al., 2017; Stephens et al., 2011, 2013).

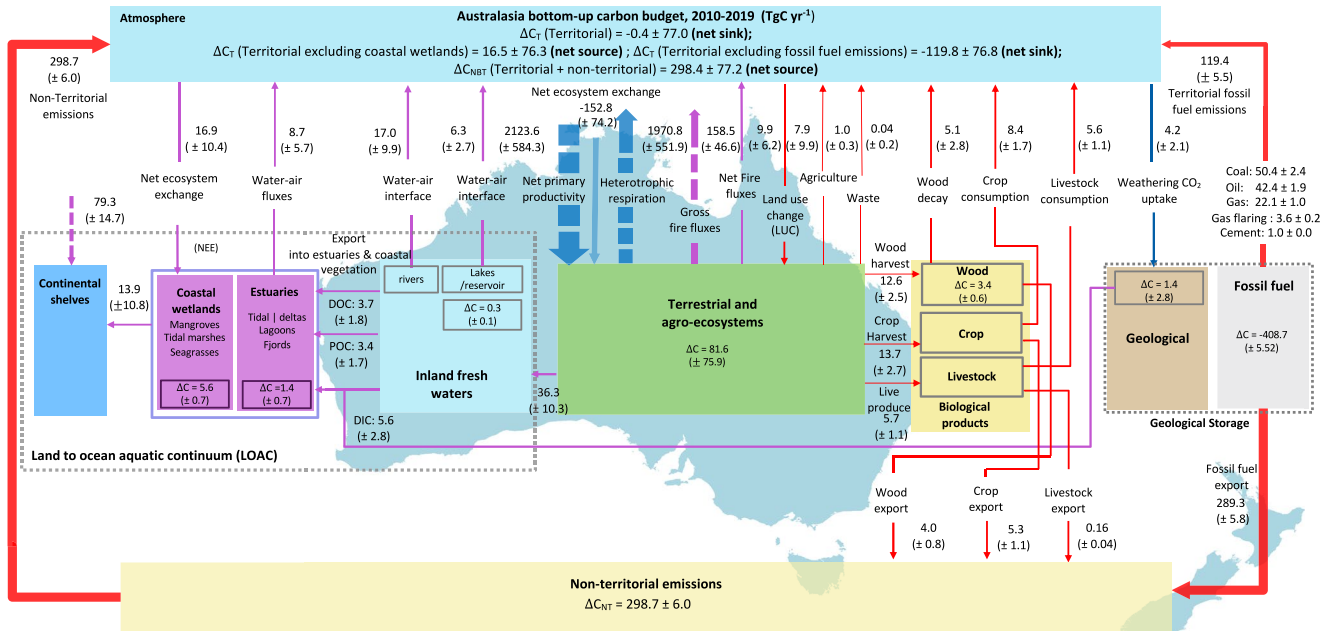
## 3. Results

### 3.1. Decadal Net Carbon Budget From the Bottom-Up Approach

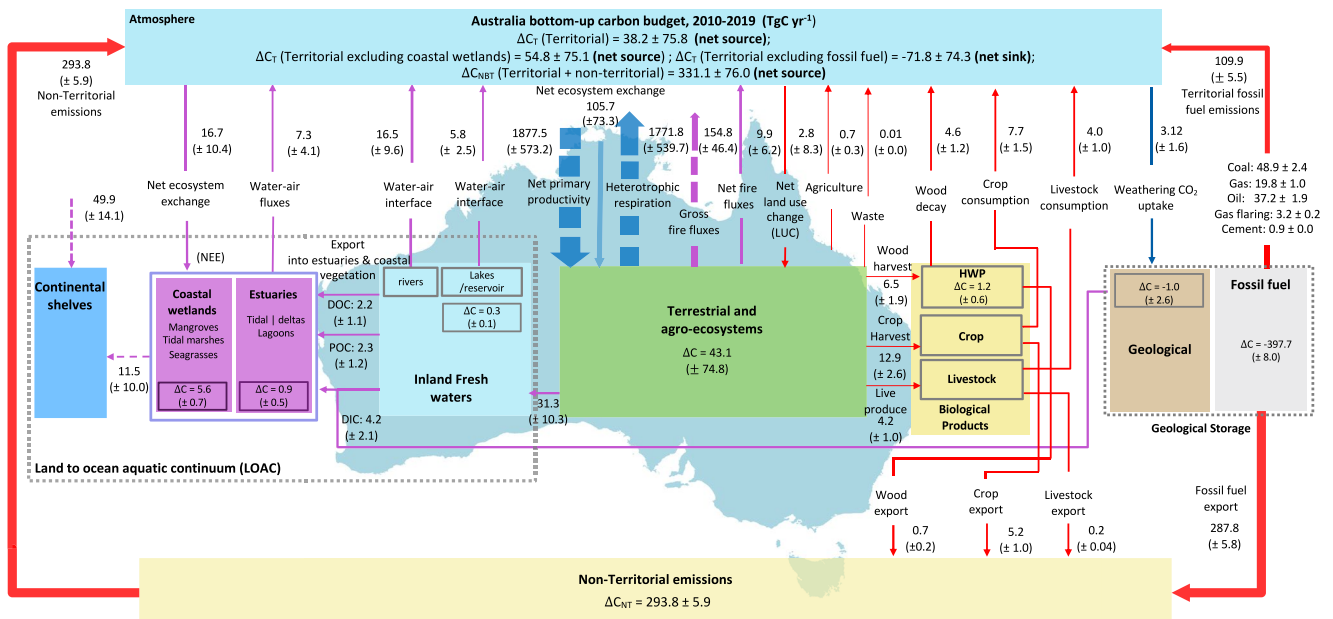
#### 3.1.1. Territorial Net Carbon Balance

Figure 2 shows the complete bottom-up carbon budget for Australasia, mean annual values for the decade 2010–2019, including all anthropogenic and natural carbon fluxes (C-CO<sub>2</sub>) in and out of the atmosphere as described in Equations 1–5 and shown in Figure 1. Fossil fuel emissions ( $119.4 \pm 6.0$  TgC yr<sup>-1</sup>; territorial component only) represent 78% of all anthropogenic net emissions, dominated by emissions from the combustion of coal





**Figure 2.** Decadal Australasia carbon budget (2010–2019). All units are in  $\text{TgC yr}^{-1}$ . The direction of fluxes is shown by the arrows; for the net  $\text{CO}_2$  balance in the atmosphere box, negative numbers indicate that the land is a  $\text{CO}_2$  sink, and positive numbers indicate that the land is a source of  $\text{CO}_2$  to the atmosphere. Red solid arrows indicate anthropogenic fluxes, blue indicates natural fluxes, and magenta indicates mixed fluxes from anthropogenic activities and natural sources. Fluxes with dash arrows are not counted as part of  $\Delta C_T$ .



**Figure 3.** Decadal Australia carbon budget (2010–2019). Details as for Figure 2.

closely followed by emissions from oil and natural gas. About 5.5% of the net anthropogenic emissions correspond to crop carbon consumption ( $8.4 \pm 1.7 \text{ TgC yr}^{-1}$ ), 3.4% livestock carbon consumption ( $5.6 \pm 1.1 \text{ TgC yr}^{-1}$ ), and 3.3% wood decay ( $5.2 \pm 2.8 \text{ TgC yr}^{-1}$ ). Other minor anthropogenic carbon fluxes that also impacted the net carbon balance were agriculture (mainly liming and urea application) ( $1.0 \pm 0.3 \text{ TgC yr}^{-1}$ ) and waste, primarily waste incineration ( $0.04 \pm 0.02 \text{ TgC yr}^{-1}$ ), contributing 0.7% of these net anthropogenic emissions.

Based on the NGHGI, we found that the land-use change flux component (excluding net fires and harvested wood products) was a small net carbon sink of  $-7.9 \pm 9.9 \text{ TgC yr}^{-1}$ . Australia contributed  $-2.8 \pm 8.4 \text{ TgC yr}^{-1}$  to this sink with the remaining (and larger) sink from New Zealand. This net  $\text{CO}_2$  sink is the result of  $\text{CO}_2$  emissions to the atmosphere from land clearing offset, several times over, by carbon sinks coming primarily from the regeneration of forests that were harvested for commercial purposes (hardwood and softwood plantations), and environmental planting (i.e., planting of native trees for biodiversity and erosion control). Regrowth of cleared land and natural regeneration also contributed to this carbon sink but to a minor degree (more details in Section 3.2.3).

Fire emissions were a net source of  $9.9 \pm 6.2 \text{ TgC yr}^{-1}$ , which included fires of anthropogenic origin (prescribed burning) and natural (wildfires) minus post-fire regeneration (forest regrowth). Analysis of the gross fire emissions determined by the GFED, GFAS, and QFED global fire emissions products (Figure S2 in Supporting Information S1) shows that, on average, Australasia released about  $158 \pm 46.6 \text{ TgC yr}^{-1}$  into the atmosphere, almost exclusively dominated by fires in Australia. New Zealand's gross fire emissions were  $3.7 \pm 4.4 \text{ TgC yr}^{-1}$ , equal to 2.3% of Australia's gross fire emissions.

We found that the largest natural flux (NEE) was  $-152.8 \pm 74.2 \text{ TgC yr}^{-1}$  during 2010–2019, showing that terrestrial ecosystems in Australasia were a large  $\text{CO}_2$  sink, offsetting 96% of the territorial fossil fuel emissions. NEE was primarily driven by the land's net primary productivity (NPP) of  $2123.6 \pm 584.3 \text{ TgC yr}^{-1}$  minus the carbon losses due to heterotrophic respiration (Rh) of  $1970.8 \pm 551.9 \text{ TgC yr}^{-1}$  (corrected for lateral export of harvest wood, crop and livestock, and river transport). Together with fossil fuels, these fluxes dominate the changes in the net territorial atmospheric  $\text{CO}_2$  balance.

We also considered  $\text{CO}_2$  fluxes from the land-to-ocean aquatic continuum (LOAC) arising from both natural and human-induced emissions. Rivers, lakes (including reservoirs) and estuaries were net  $\text{CO}_2$  sources to the atmosphere of  $17.0 \pm 9.9 \text{ TgC yr}^{-1}$ ,  $6.2 \pm 2.7 \text{ TgC yr}^{-1}$  and  $8.7 \pm 5.7 \text{ TgC yr}^{-1}$ , respectively. Together, these three sources were partly compensated by the uptake of atmospheric  $\text{CO}_2$  into tidal wetlands and submerged vegetation ( $-16.9 \pm 10.4 \text{ TgC yr}^{-1}$ ). Other LOAC fluxes, such as the carbon transported by rivers to the coastal ecosystem, were estimated to be  $12.7 \pm 0.7 \text{ TgC yr}^{-1}$ . We estimated by mass balance that the total amount of carbon transported from coastal ecosystems to continental shelves was  $13.9 \pm 10.8 \text{ TgC yr}^{-1}$ . Carbon burial rates in estuaries and coastal wetlands were  $5.6 \pm 0.7$  and  $1.4 \pm 0.7 \text{ TgC yr}^{-1}$ , respectively.

By combining all anthropogenic and natural carbon sources and sinks (excluding non-territorial emissions), we found that the mean of Australasia's net territorial carbon balance (CT) was close to carbon neutral ( $-0.4 \pm 77.0 \text{ TgC yr}^{-1}$ ). As shown in Figures 3 and 4, Australasia's carbon neutrality during 2010–2019 was largely because the dominant fossil fuel source of  $\text{CO}_2$  emissions was offset by the biospheric carbon sinks (show the total sink here). While Australia's land was the largest contributor ( $-128.3 \pm 74.5 \text{ TgC yr}^{-1}$ ), New Zealand's sink contribution ( $-53.5 \pm 17.5 \text{ TgC yr}^{-1}$ ) is more significant per unit area considering that the area of New Zealand represents only 4% of Australia's land area. While Australia's land was the larger contributor to the Australasia carbon sink, New Zealand's sink contribution is more significant per unit area considering that the area of New Zealand represents only 4% of Australia's land area. In contrast to the Australasia carbon neutrality, Australia was a carbon source of  $38.2 \pm 75.8 \text{ TgC yr}^{-1}$ , and New Zealand a carbon sink of  $-38.6 \pm 13.4 \text{ TgC yr}^{-1}$ . Australia was a source of carbon because fuel emissions represent the largest source of emissions (70%) among all natural and anthropogenic sources.

### 3.1.2. Non-Territorial and the Net Atmospheric Total Carbon Balance

Australasia's non-territorial carbon emissions (i.e., those emissions embedded in fossil fuel, wood, crops, and livestock exported and consumed overseas) were  $298.7 \pm 6.0 \text{ TgC yr}^{-1}$ . Australia contributed almost the entire quantity of these emissions ( $293.3 \pm 5.8 \text{ TgC yr}^{-1}$ ), while Zealand's only contributed  $3.9 \pm 1.1 \text{ TgC yr}^{-1}$ .

As seen in Figure 2, Australasia's non-territorial fossil fuel emissions were 2.4 times larger than territorial fossil fuel emissions. Under the UNFCCC, non-territorial emissions are not part of the country of origin but are the

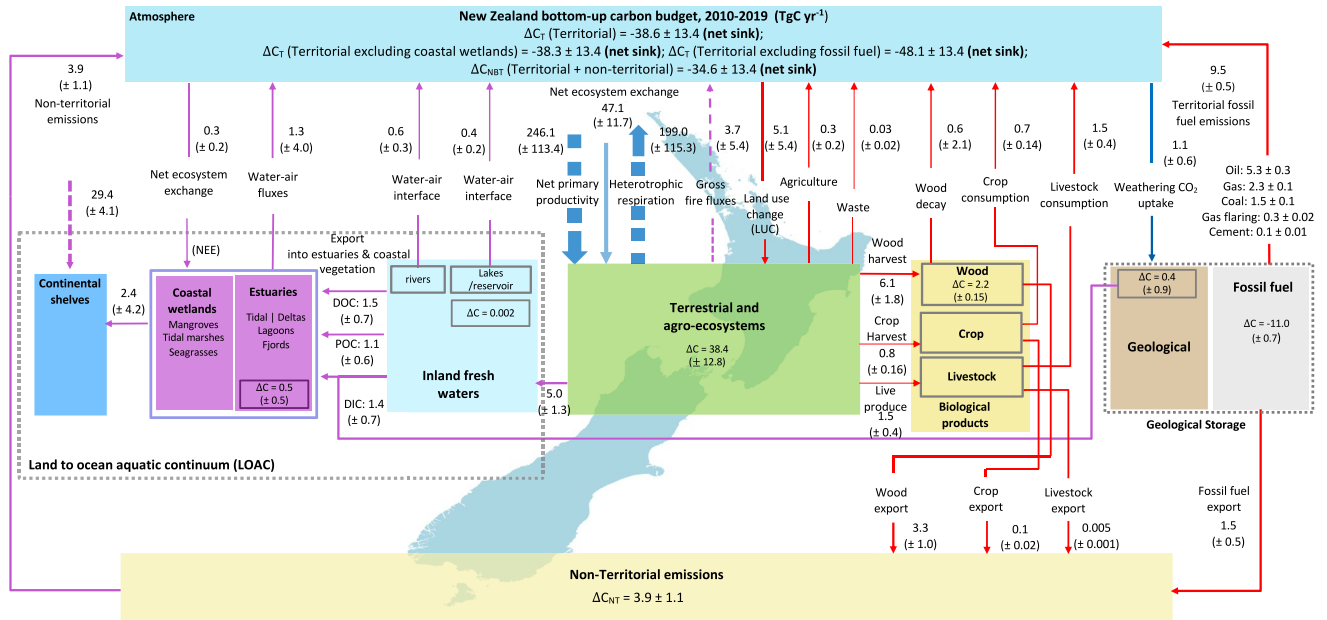


Figure 4. Decadal New Zealand carbon budget (2010–2019). Details as for Figure 2.

responsibility of the importer country where they are consumed (e.g., burn the fossil fuels or eat the food products). An exception is harvested wood products (HWPs), for which emissions are often linked to the location of the harvested forest.

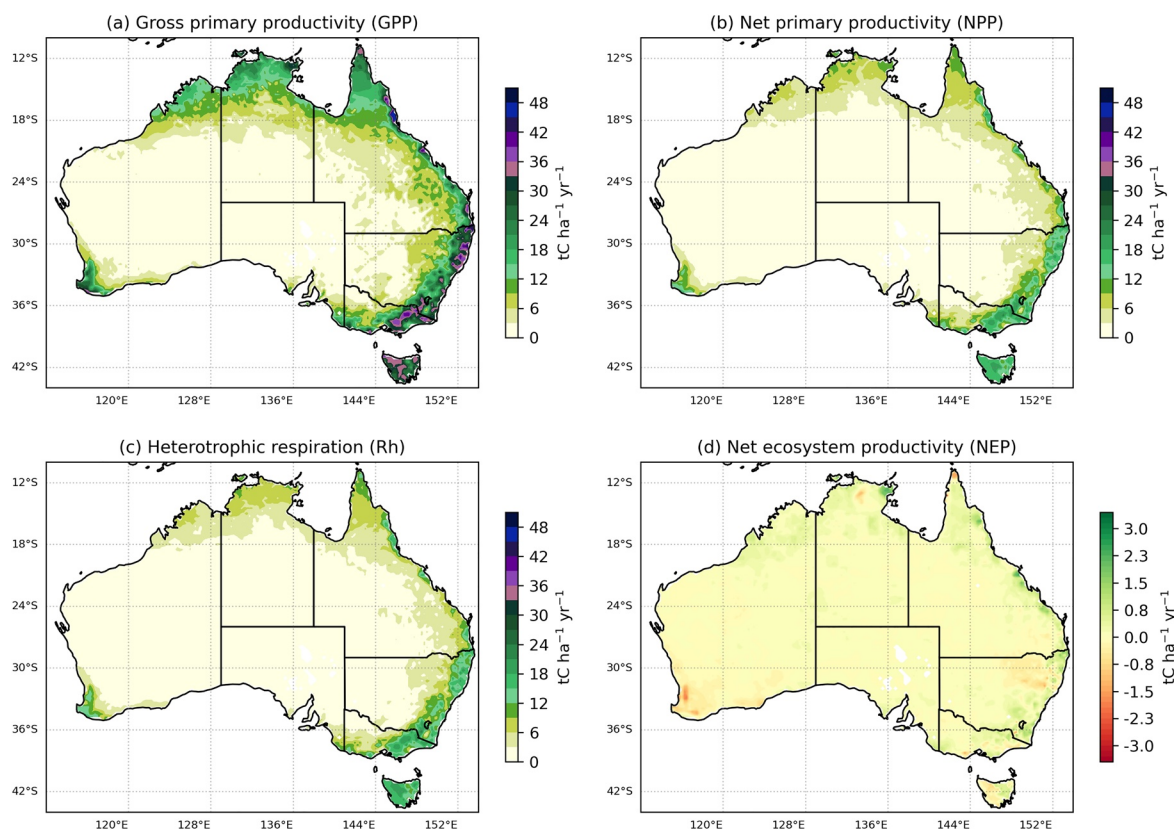
Counting both territorial and non-territorial emissions, Australia and New Zealand's net atmospheric CO<sub>2</sub> contribution ( $\Delta C_A$ ) were  $331.9 \pm 76.0$  TgC yr<sup>-1</sup>, and  $-34.6 \pm 13.4$  TgC yr<sup>-1</sup> respectively, with a total net contribution of  $298.4 \pm 77.2$  TgC yr<sup>-1</sup> for Australasia.

### 3.2. Major Flux Components of the Bottom-Up Carbon Budget

#### 3.2.1. Biosphere Carbon Flux Estimates

Figure 5 shows the spatial distribution of Australia's major carbon fluxes from the biosphere (GPP, NPP, Rh, and NEP, which is the equivalent to the NEE in Figure 2) averaged from 2010 to 2019 (without external disturbances such as fires, harvest, LUC or fluxes influenced in the LOAC ecosystem). Most of the plant productivity (GPP; Figure 5a) is concentrated along the eastern, northern and south-western coast and immediate hinterland of the continent ( $2.4$ – $4.8$  tC ha<sup>-1</sup> yr<sup>-1</sup>), with very low GPP values in the interior ( $<0.3$  tC ha<sup>-1</sup> yr<sup>-1</sup>). NPP is about half of the GPP (Figure 5b) and values along the coast are around  $1$ – $2$  tC ha<sup>-1</sup> yr<sup>-1</sup>.

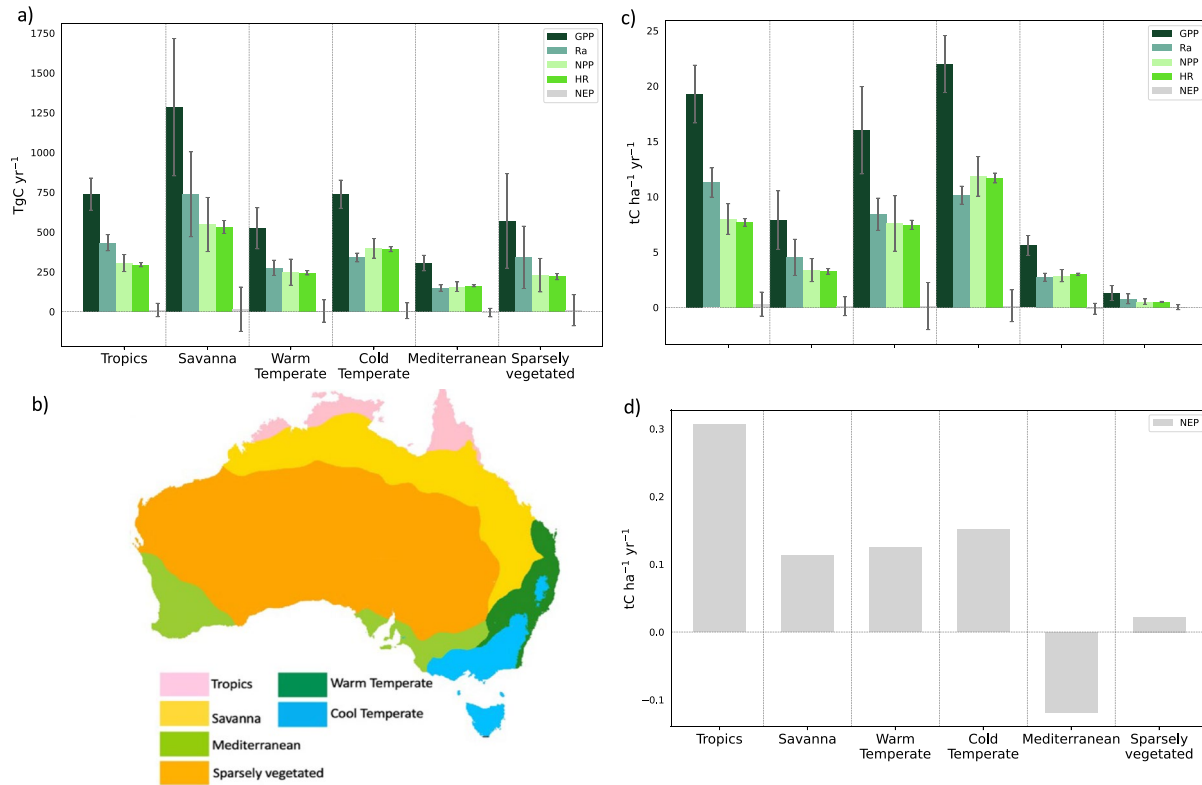
To better understand the size of NEP carbon fluxes across Australian ecosystems, we aggregated these fluxes into six different bioclimatic classes: tropical, savanna, warm temperate, cool temperate, Mediterranean, and sparsely vegetated (Figure 6). We found that NEP over semi-arid ecosystems such as savanna and sparsely vegetated (Figure 6a) were  $15.5 \pm 139.4$  (1 $\sigma$ ) TgC yr<sup>-1</sup> and  $9.1 \pm 97.6$  (1 $\sigma$ ) TgC yr<sup>-1</sup>, respectively, compared to the tropics ( $10.5 \pm 42.0$  (1 $\sigma$ ) TgC yr<sup>-1</sup>), warm temperate ( $4.5 \pm 69.7$  (1 $\sigma$ ) TgC yr<sup>-1</sup>), and cold temperate regions ( $5.9 \pm 49.4$  (1 $\sigma$ ) TgC yr<sup>-1</sup>). Figure 6d shows that the largest NEP found in semi-arid ecosystems is due to the large extent of these regions, and not to high vegetation productivity; we define semi-arid ecosystems here as those including savanna and sparse vegetation (rangelands) that covers approximately 80% of the continent. Figure 6d shows that cold and warm temperate ecosystems and tropical areas were the most productive vegetation in the continent per unit area with tropical NEP of  $0.3 \pm 0.9$  tC ha<sup>-1</sup> yr<sup>-1</sup> and sparsely vegetated NEP of  $0.02 \pm 0.2$  tC ha<sup>-1</sup> yr<sup>-1</sup>.



**Figure 5.** Decadal average (2010–2019) of (a) GPP, (b) NPP, (c) Rh, and (d) NEP carbon fluxes obtained from CABLE-BIOS3 simulations over Australia. NEP and NPP represent productivity, therefore, a positive sign means uptake by land, and a negative sign represents carbon release to the atmosphere). Units  $\text{tC ha}^{-1} \text{yr}^{-1}$  refers to tonnes of carbon per hectare per year.

Although on a per-area basis, semi-arid ecosystems were not as productive on a per-area basis as the tropical ecosystems, they nonetheless contributed as much to the continental carbon sink as the more productive biomes because of their much greater area extent. Semi-arid regions also exhibited much more variable sink activity (Figure S12 in Supporting Information S1), with the years 2010, 2011, 2016, and 2017 being particularly productive (data not shown). Overall, Australia was a strong sink in 2011, mostly driven by high precipitation over much of the continent due to a strong La Niña (Figure S13 in Supporting Information S1).

New Zealand's modeled carbon fluxes from the biosphere (GPP, NPP, Rh and NEP) averaged over 2010–2019 are shown in Figure 7. New Zealand's process-based model (Biome-BGC Muso and CenW) estimates indicate that most of New Zealand was a net carbon sink. Forested areas (Figure S14 in Supporting Information S1) in the northern part of the North Island (plantation pine forest) and the west coast of the South Island (native evergreen broadleaf forest) were particularly productive, with GPP of  $4.0\text{--}4.3 \text{ tC ha}^{-1} \text{ year}^{-1}$ . These regions have favorable growing conditions, with temperatures above freezing year-round and ample precipitation (NIWA, 2023). The northern and western areas of the North Island include highly productive managed grasslands that are typically grazed by dairy cows (Figure S14 in Supporting Information S1). These ecosystems are also modeled as  $\text{CO}_2$  sinks from a biosphere perspective. However, most of the carbon in the grass consumed by the animals is either respired back to the atmosphere or exported as milk and meat products, rendering whole pastoral farming systems in New Zealand close to carbon- $\text{CO}_2$ -neutral in its territory, with emissions of  $2.34 \pm 0.81 \text{ TgC yr}^{-1}$  (see e.g., (Hunt et al., 2016; Wall et al., 2019). Note that we have not included carbon released as methane as part of animal digestive processes in this C- $\text{CO}_2$  budget. The lower North Island and the eastern part of the South Island are less productive but are still modeled to be small net sinks ( $\text{NEP} \sim 0.1\text{--}0.2 \text{ tC ha}^{-1} \text{ yr}^{-1}$ ). These areas are dominated by low-productivity grasslands on rolling hills prone to erosion and are often used to graze sheep and/or beef cattle. Alpine grasses (tussock) and tundra in the Southern Alps that run along the middle of the South Island are modeled as a small net source, likely due to the high elevation, poor soils and marginal growing conditions.



**Figure 6.** (a) Australia's gross primary productivity (GPP), autotrophic respiration (Ra), net primary productivity (NPP), heterotrophic respiration (Rh) and net ecosystem productivity (NEP) aggregated over (b) six different bioclimate regions (tropics, savanna, Mediterranean, sparsely vegetated, warm temperate and cool temperate) for 2010–2019. (c) Same as in panel (a) but divided by the hectare of each Australian bioclimate region (units  $\text{tC ha}^{-1} \text{yr}^{-1}$  refers to tonnes of carbon per hectare per year). Uncertainties in (a) and (c) represent the annual variability (standard deviation) of the CABLE-POP simulations. Panel (d) corresponds to the NEP aggregated over the bioclimate regions shown in panel (b). To better demonstrate the size of the NEP flux in each bioclimatic region, no uncertainties are included in panel (d). Units in panel (d) are the same as in panel (c).

Although New Zealand spans a large latitudinal range ( $35^{\circ}$ – $46^{\circ}\text{S}$ ) with very different temperature and rainfall patterns, under the bioclimatic classification system shown for Australia in Figure 6, New Zealand is classified almost entirely as “cool temperate,” so we have not attempted to analyze the fluxes by bioclimatic zones.

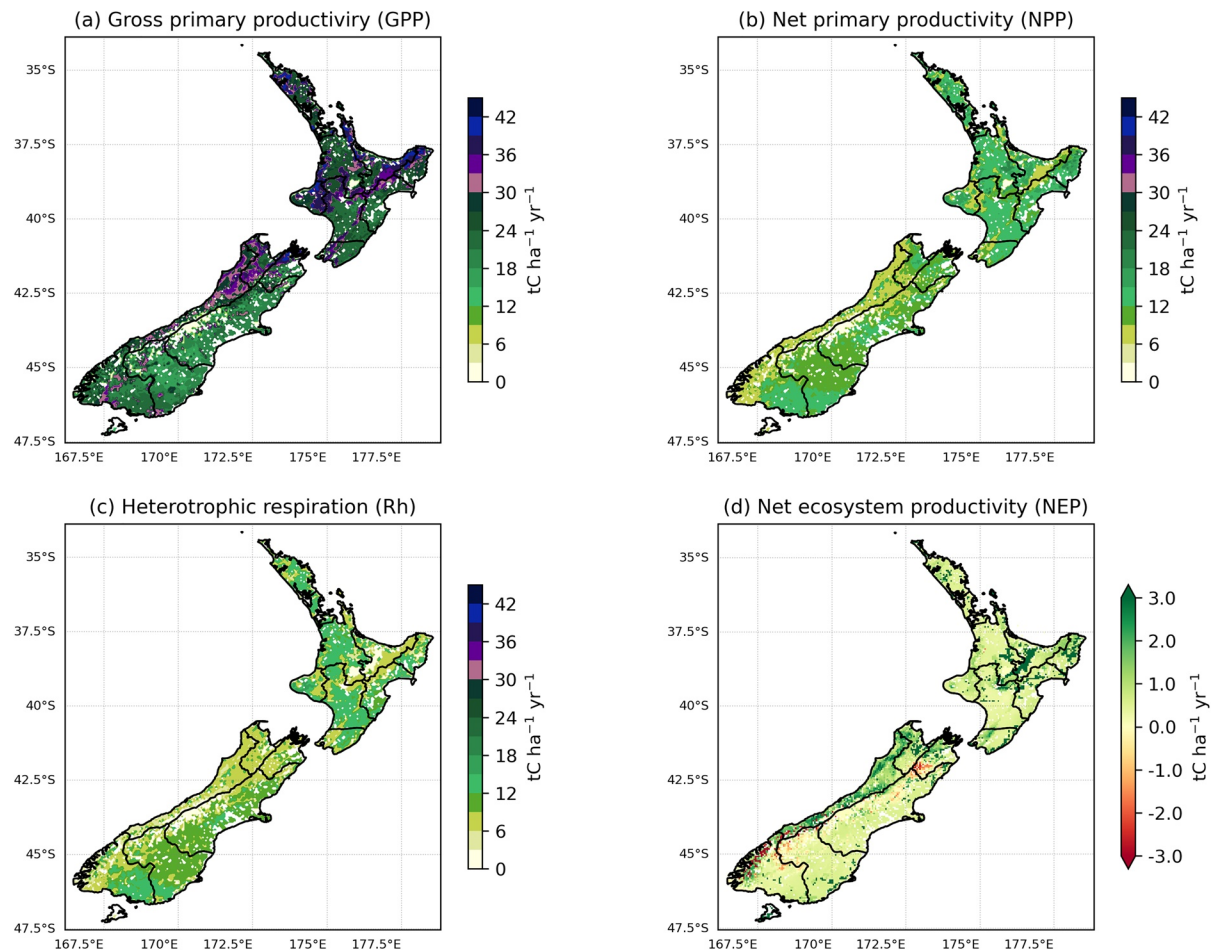
New Zealand's biosphere is consistently a net carbon sink from year to year (Figure S15 in Supporting Information S1). There is some regional variation, mainly driven by the interannual variation in precipitation, especially in drier regions (eastern areas of both islands). Some of this variation is mitigated by irrigation and management of pasture. However, our modeling results suggest that in general, New Zealand's temperate climate supports highly productive natural and managed biomes.

### 3.2.2. Fire Emissions

Australasia's gross fire emissions were  $158.5 \pm 46.6 \text{ TgC yr}^{-1}$  (Figure S3a in Supporting Information S1) for the decade of 2010–2019, of which most emissions ( $154.8 \pm 4.4 \text{ TgC yr}^{-1}$ ) (98%) came from Australia. Considering Australia's post-fire vegetation regrowth, the net fire emissions in this region were  $9.9 \pm 5.1 \text{ TgC yr}^{-1}$ . New Zealand's biomass burning (i.e., wildfires and controlled burning) is not a significant source of emissions because controlled burning is limited, and wildfires are rare due to New Zealand's cool temperate climate and vegetation. Here, therefore, we only present results for Australia, which are restricted to temperate forests and tropical savanna ecosystems (Text S3.1 in Supporting Information S1).

Australia's temperate forests and their burning/regrowth dynamics differ from a tropical savanna because gross fire emissions from forests can be several times as large as the regrowth on an annual time scale and therefore act as strong carbon sources (as seen in 2002, 2006, and 2019, Figure S2a in Supporting Information S1). For the





**Figure 7.** Decadal average (2010–2019) of (a) GPP, (b) NPP, (c) Rh and (d) NEP carbon fluxes obtained from Biome-BGCMuSo (dairy, sheep pasture and EBF/indigenous forest) and CenW (exotic forest-pine and shrub-mānuka/kānuka) simulations over New Zealand. NEP and NPP represent productivity; therefore, a positive sign means an uptake by land, and a negative sign represents carbon release to the atmosphere. Units  $\text{tC ha}^{-1} \text{yr}^{-1}$  refers to tonnes of carbon per hectare per year.

last decade, the net fire emissions recorded in this region were very large ( $12.9 \pm 4.32 \text{ TgC yr}^{-1}$ ), while tropical savannas were a net sink ( $2.95 \pm 0.8 \text{ TgC yr}^{-1}$ ) (Figures S2a and S2b in Supporting Information S1). Savanna fires are dominated by the burning of its herbaceous component whose carbon stocks are much faster to recover after fire than high carbon density forests in temperate regions. We note that the large net carbon source recorded in the last decade for temperate forests was primarily driven by the 2019 fires ( $133.7 \pm 44.8 \text{ TgC yr}^{-1}$ ).

### 3.2.3. Land Use Change (LUC)

Australasia's land use change  $\text{CO}_2$  fluxes, excluding Australia and New Zealand's HWP (Section 3.2.5) and net fire emissions for Australia (Section 3.2.2), was a carbon sink to the land of  $-7.9 \pm 9.9 \text{ TgC yr}^{-1}$ . This net carbon sink has two opposing fluxes: (a) an emission component associated with land clearing and the conversion of forest to cropland or grassland ( $12.6 \pm 6.1 \text{ TgC yr}^{-1}$ ), and (b) a sink component associated with afforestation, reforestation and forest management ( $-21.3 \pm 7.7 \text{ TgC yr}^{-1}$ ) that outweighed the  $\text{CO}_2$  sources. Australia and New Zealand's sinks contributed  $-14.6 \pm 5.5 \text{ TgC yr}^{-1}$  (68%) and  $-6.8 \pm 5.4 \text{ TgC yr}^{-1}$  (32%) to Australasia's LUC respectively. A large part of Australia's carbon sinks came from the establishment of new commercial plantations (hardwood and softwood) ( $-5.7 \pm 0.85 \text{ TgC yr}^{-1}$ ) and regrowth on previously cleared forest lands ( $-3.3 \pm 0.56 \text{ TgC yr}^{-1}$ ). A minor part ( $-0.1 \pm 0.02 \text{ TgC yr}^{-1}$ ) of Australia's LUC sink came from forest regrowth after cropland abandonment (e.g., land abandoned after agricultural and pastoral clearing).

New Zealand's net  $\text{CO}_2$  sink ( $-5.1 \pm 5.4 \text{ TgC yr}^{-1}$ ) came mostly from the growth and re-growth of forest on existing managed forest land ( $-3.7 \pm 2.9 \text{ TgC yr}^{-1}$ ). New Zealand's exotic plantation forests have some of the highest growth rates in the world due to its temperate climate, abundant rainfall and fertile soils (New Zealand Ministry

for the Environment, 2021). The sink from forest growth and harvested wood products more than compensated for emissions from harvesting. There was also a small contribution to the overall sink from the afforestation of grassland. Conversely, forest land converted to grassland and changes in management practices on grassland contributed a small source, on the same order of magnitude as the sink from grasslands converted to forest. Overall, emissions and removals from land-use change were outweighed by the sink from existing forest land.

### 3.2.4. Land to Ocean Aquatic Continuum (LOAC) Carbon Fluxes

#### 3.2.4.1. Inland Water Emissions

Inland aquatic ecosystems receive large inputs of DOC, DIC, and POC from soils and vegetation and emit a substantial amount of CO<sub>2</sub> to the atmosphere. Figure 8a shows that rivers release more CO<sub>2</sub> into the atmosphere compared to natural lakes, reservoirs, and lakes regulated by dams in Australasia. The river flux median rate (17.4 [6.5–26.9] (min-max)) represents 80% of all inland aquatic CO<sub>2</sub> emissions. Natural lakes were the second largest emitter and represented 18% of all inland aquatic CO<sub>2</sub> emissions, with a median emission rate of 3.9 [3.5–8.6] TgC yr<sup>-1</sup>. Minor CO<sub>2</sub> emissions were found from reservoirs, with a median flux of 0.6 [0.3–0.9] TgC yr<sup>-1</sup>, and from dams (0.1 [0.1–0.2] TgC yr<sup>-1</sup>). The small contribution of these two ecosystems is related to the surface area, which only represents 7% (3,816 km<sup>2</sup>) and 1% (1,128), respectively, compared to the total surface area of the natural lakes (51,666 km<sup>2</sup>) (Figure S6 in Supporting Information S1).

Based on the Australia NGHGI, CO<sub>2</sub> emissions from human-made reservoirs were 0.1 TgC yr<sup>-1</sup> for 2010–2019. We subtracted this estimate from the reservoir emission rates calculated from HydroLakes to avoid double-counting.

#### 3.2.4.2. Estuaries

Estuaries such as tidal systems and deltas, lagoons, and fjords (Figure 1) receive large amounts of DIC, DOC and POC from rivers and underground flows, resulting in a source of CO<sub>2</sub> to the atmosphere (Figure 8b). The median estimate of these aquatic ecosystems across Australasia was 7.5 [–0.3–38.3] TgC yr<sup>-1</sup>. Tidal systems and deltas were the main source of CO<sub>2</sub> emissions, with a median flux of 5.5 [–0.3–0.4] TgC yr<sup>-1</sup>.

The organic carbon deposition rate ( $\Delta C_{ES}$  burial) into estuarine sediments in Australasia was  $1.4 \pm 0.7$  TgC yr<sup>-1</sup>. From this estimate, Australia accounts for 64% ( $0.9 \pm 0.5$  TgC yr<sup>-1</sup>), and New Zealand 36% ( $0.5 \pm 0.2$  TgC yr<sup>-1</sup>).

#### 3.2.4.3. Coastal Wetlands

In contrast to estuaries, coastal wetlands (mangroves, salt marshes and seagrasses; also referred to as blue carbon) act as net ecosystem CO<sub>2</sub> sinks across Australasia (Figure 8c). Based on the sum of medians, the net ecosystem exchange (NEE) for coastal wetlands was estimated at  $-16.7$  [–18.3–3.8] TgC yr<sup>-1</sup>. The largest contributors to this carbon sink were mangroves (43%) and seagrasses (40%). Australia was responsible for about 98% of the sink, with a median-estimated value of  $-16.4$  [–18.3–3.8] TgC yr<sup>-1</sup>. New Zealand's coastal wetland sink was  $-0.27$  [–0.37–0.02] TgC yr<sup>-1</sup>.

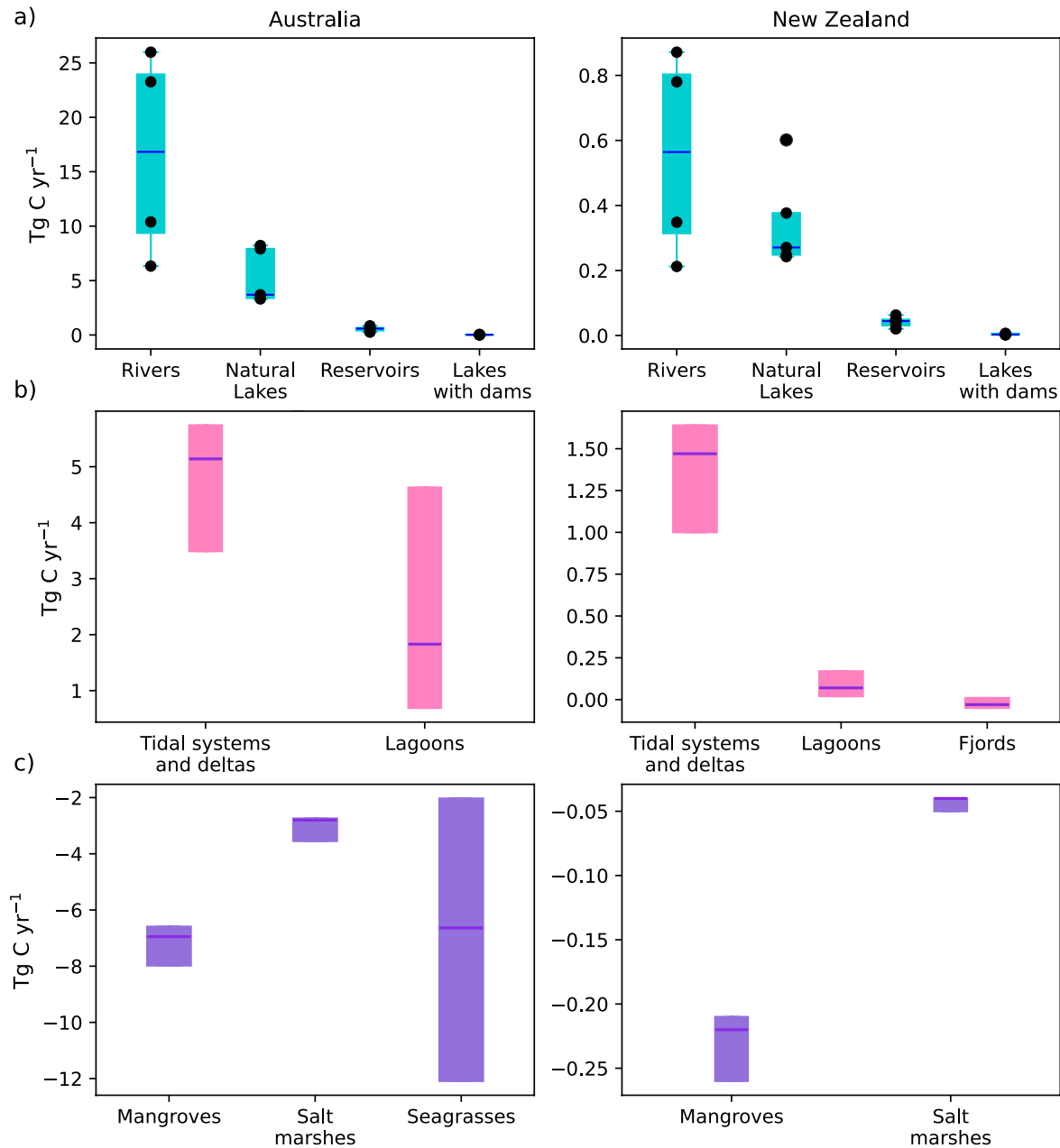
Australia's organic carbon sequestration rates ( $\Delta C$  burial) for coastal wetlands were estimated at  $-5.6 \pm 0.7$  TgC yr<sup>-1</sup> (Figure 3). Based on a review of existing literature, we found that the carbon burial rates of seagrasses, mangroves, and salt marshes in Australia were  $3.6 \pm 0.7$  TgC yr<sup>-1</sup>,  $1.5 \pm 0.1$  TgC yr<sup>-1</sup>, and  $0.5 \pm 0.1$  TgC yr<sup>-1</sup> respectively.

Carbon sequestration rates in kelp forests in Australia have been suggested to be 30% of the total blue carbon stored and sequestered around the Australian continent (e.g., Filbee-Dexter & Wernberg, 2020) with recent estimates of  $1.3$ – $2.8$  TgC yr<sup>-1</sup>. We did not include this estimate in the budget because part of the carbon sequestered by kelp forests is exported to the open ocean, and the fraction that sinks to the ocean's floor and becomes a long-term sink is still highly uncertain.

### 3.2.5. Territorial and Non-Territorial Carbon Emissions From Crops, Wood, and Livestock, and Lateral Fluxes

Territorial emissions due to wood decay were  $5.2 \pm 2.8$  TgC yr<sup>-1</sup>, similar to those embedded in wood products exported overseas (non-territorial emissions of  $4.0 \pm 0.8$  TgC yr<sup>-1</sup>). New Zealand was responsible for most of these exported emissions ( $3.4$  TgC yr<sup>-1</sup>), being 2.3 times higher than Australia; 65% of the total wood emissions took place overseas (non-territorial).

Carbon emissions associated with the national demand of crops were  $8.4 \pm 1.7$  TgC yr<sup>-1</sup>, 1.5 times higher than the emissions exported and consumed overseas ( $5.3 \pm 1.1$  TgC yr<sup>-1</sup>). Barley, rapeseed, and wheat constituted



**Figure 8.** (a) Inland CO<sub>2</sub> emissions from rivers, natural lakes, reservoirs, and lakes regulated by dams in Australia, and New Zealand; black dots represent CO<sub>2</sub> estimates from peer-reviewed published studies (as reviewed in Lauerwald et al. (2023); Table S1 in Supporting Information S1) upscaled to Australia and New Zealand by the surface area of inland water bodies within these two regions. (b) Estuaries water-air CO<sub>2</sub> emissions from tidal systems and deltas, lagoons, and fjords (Rosentreter et al., 2023) (c) Net Ecosystem Exchange (NEE) of coastal vegetation wetlands (mangroves, salt marshes, seagrasses) (Rosentreter et al., 2023). Boxplot in (b) and (c) shows the median (violet blue line) and interquartile (Q1-Q3) range of estuaries and coastal wetlands CO<sub>2</sub> gas exchange.

60% of all crop emissions exported and consumed abroad, where Australia was the main (98%) exporter of these emissions at  $5.2 \pm 1$  TgC yr<sup>-1</sup>; New Zealand contributed 0.11 TgC yr<sup>-1</sup>.

National livestock carbon emissions associated with the consumption of livestock products were  $5.5 \pm 1.1$  TgC yr<sup>-1</sup>, where the highest carbon emissions were due to consumption of products derived from cattle ( $4.0 \pm 1.0$  TgC yr<sup>-1</sup>) (40%), and sheep ( $1.1 \pm 0.28$  TgC yr<sup>-1</sup>) (20%). Non-territorial livestock emissions were found to be considerably lower in comparison with the national average ( $0.16 \pm 0.04$  TgC yr<sup>-1</sup>).

Lateral fluxes of HWP ( $12.6 \pm 2.5$  TgC yr<sup>-1</sup>), crops ( $13.7 \pm 2.7$  TgC yr<sup>-1</sup>), and livestock products ( $5.7 \pm 1.1$  TgC yr<sup>-1</sup>) were subtracted from the heterotrophic respiration flux estimate simulated by the land surface models to avoid double counting of these emissions.

### 3.2.6. Territorial and Non-Territorial Fossil Fuel Emissions

Australasia's total territorial and non-territorial CO<sub>2</sub> fossil fuel emissions were  $119.4 \pm 5.5$  TgC yr<sup>-1</sup>, and  $289.3 \pm 5.8$  TgC yr<sup>-1</sup>, respectively. Australia alone represented 92% ( $109.9 \pm 5.5$  TgC yr<sup>-1</sup>) of territorial fossil fuel emissions and almost all ( $287.8 \pm 5.8$  TgC yr<sup>-1</sup>) of the fossil fuel exported and burned overseas.

Australia's territorial CO<sub>2</sub> emissions from extraction and use of fossil fuel (coal, oil and gas) were responsible for 45% ( $48.9 \pm 2.4$  TgC yr<sup>-1</sup>), 34% ( $37.2 \pm 1.9$  TgC yr<sup>-1</sup>), and 18% ( $19.8 \pm 1.0$  TgC yr<sup>-1</sup>) of all territorial fossil fuel CO<sub>2</sub> emissions (Figure S10a in Supporting Information S1). For New Zealand, fossil fuel emissions were dominated by oil 55% ( $5.3 \pm 0.26$  TgC yr<sup>-1</sup>) and gas ( $0.3 \pm 0.02$  TgC yr<sup>-1</sup>) 24%, respectively (Figure S10b in Supporting Information S1).

Australia's non-territorial fossil fuel contribution was mainly due to the export of thermal ( $124.2 \pm 4.0$  TgC yr<sup>-1</sup>) and metallurgical coal ( $126.8 \pm 4.1$  TgC yr<sup>-1</sup>), which together represent 87% of total Australasia fossil fuel export (Figure S10b in Supporting Information S1). Other important sources of emissions come from exports of liquefied natural gas ( $30.15 \pm 0.7$  TgC yr<sup>-1</sup>) and crude oil ( $5.9 \pm 0.02$  TgC yr<sup>-1</sup>), which combined contributed 12% to non-territorial fossil fuel emissions.

### 3.3. Top-Down Net Carbon Balance (an Atmospheric Perspective)

Figure 9 shows a set of nine independent global/regional flux inversions compared to the bottom-up carbon budget built in this study. Here we assess the level of agreement between the inversions, and in Section 4.2, we discuss how well atmospheric inversions compare with the bottom-up estimates.

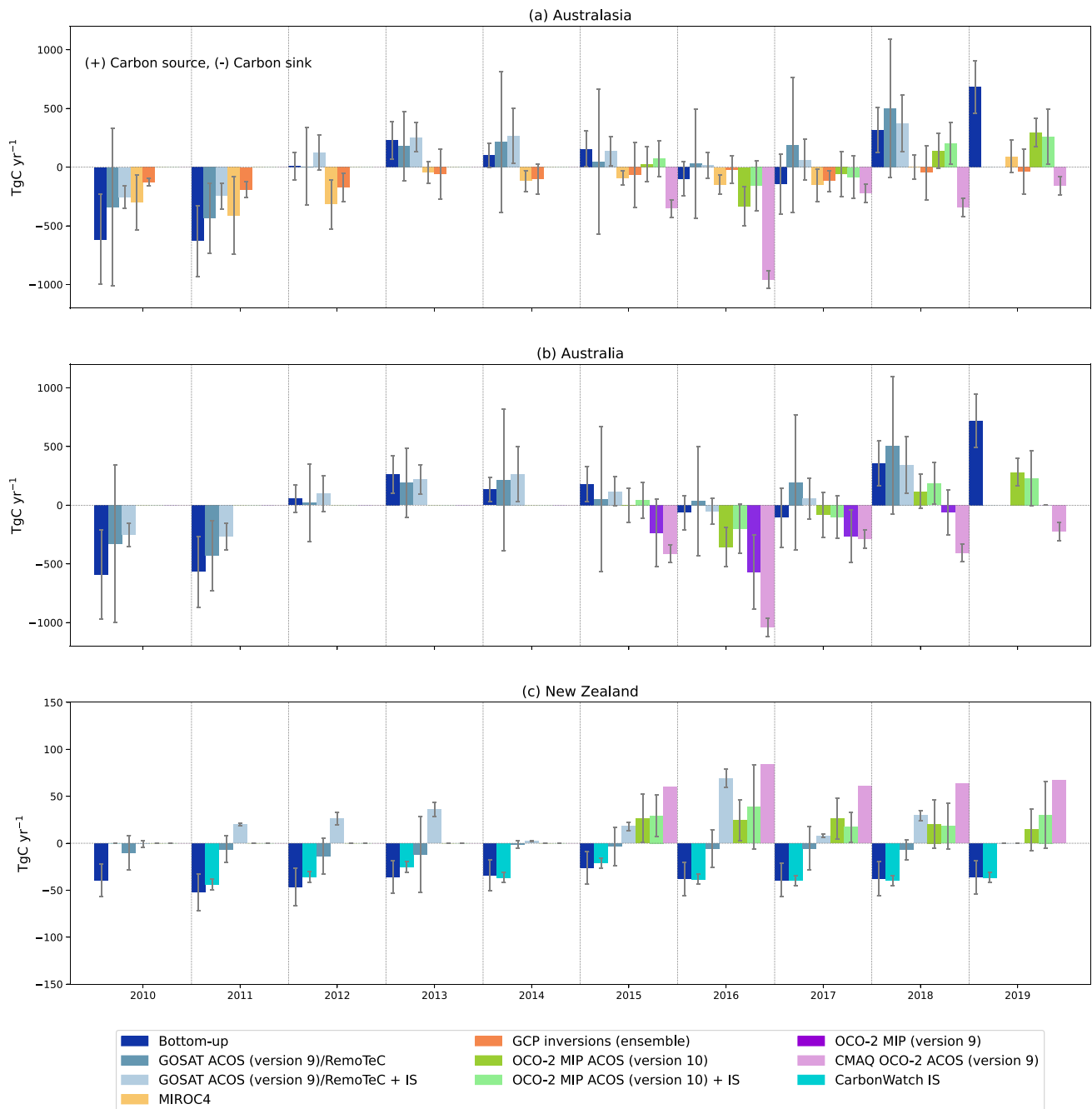
Figure 9a shows that for some years from 2015 to 2019, there is some level of consistency between Australasia's satellite/in situ derived fluxes, considering the range of uncertainties. For 2010 and 2011, GOSAT inversions agreed with in situ inversions from the GCP and MIROC4-ACTM, showing that Australasia was a carbon sink. Likewise, for the years 2018 and 2019, most inversions (GOSAT and OCO-2 MIP; ACOS, version 10) agree that Australasia acted as a source of carbon, except for OCO-2 CMAQ that shows that Australasia was a CO<sub>2</sub> sink. Differences in CMAQ is likely associated with the use of a previous version of NASA's retrieval algorithm (ACOS version 9). A few ppm of bias in OCO-2 estimates derived from the ACOS version 9 retrieval algorithm (Peiro et al., 2022) could have prevented this regional inversion from estimating the true flux, among other factors, such as the errors in the transport of the model. Australian flux inversion (Figure 9b) shows similar findings to Australasia. It is likely that the Australasia/Australia satellite flux inversion based on the latest satellite retrievals of OCO-2 (ACOS version 10), as will be shown in Section 4.3, provides the best independent and closer estimate to the net carbon balance (bottom-up budget) estimated in this study.

New Zealand's National scale flux inversion (Figure 9c) shows poor agreement with GOSAT, OCO-2 MIP, and CMAQ OCO-2 satellite-based inversions. New Zealand's national inversion suggests that this country acted as a carbon sink from 2015 to 2019 of  $44 \pm 7$  TgC yr<sup>-1</sup>, while all other satellite inversions show a carbon source of 25 TgC yr<sup>-1</sup> with a range from 17 to 30 TgC yr<sup>-1</sup>. We place a low confidence level on satellite flux inversions over New Zealand because the number of soundings, either GOSAT or OCO-2, over this country is limited, and the temporal resolution is low (e.g., OCO-2 has an approximate 16 days re-visit cycle with sounding at around 13:30 local time).

## 4. Discussion

### 4.1. Bottom-Up Carbon Budget of Australasia

Our decadal bottom-up territorial carbon assessment, including all-natural and anthropogenic fluxes, suggests that Australasia was close to carbon neutral, with large uncertainties. This carbon neutrality was achieved because the terrestrial biospheric CO<sub>2</sub> sink offsets most anthropogenic emissions from this region. Previous studies attribute the Australian and global land CO<sub>2</sub> sinks largely to the existence of a long-term sink driven by the CO<sub>2</sub> fertilization effect on vegetation growth (Canadell, Costa, et al., 2021; Canadell, Meyer, et al., 2021; Haverd



**Figure 9.** Australasia (a), Australia (b), New Zealand's (c) multi-year annual mean  $\text{CO}_2$  flux based on this assessment (bottom-up) with top-down estimations using satellite-based inversions using GOSAT (ACOS/RemoTeC)/OCO-2 (ACOS), and MIROC4 and GCP inversions (Friedlingstein et al., 2020). Annual bottom-up estimates correspond to net carbon flux ( $\Delta C_T$ ) shown in Figure 1. Error bars in the bottom-up and top-down approaches are described in Table 1. We note that error bars in the bottom-up flux estimates represent the square-root of the linear sum of squared uncertainty components of the budget shown in Figure 1.

et al., 2013, 2020; Teckentrup et al., 2021; Walker et al., 2021). Such an effect is the result of the excess  $\text{CO}_2$  that has been accumulating in the atmosphere over the past 200 years from the combustion of fossil fuels and land use (Canadell, Costa, et al., 2021; Canadell, Meyer, et al., 2021; Friedlingstein et al., 2022). This  $\text{CO}_2$  accumulation has led to an increase in the rate of carbon fixation by photosynthesis of around 30% since 1900 (Haverd et al., 2020).

We also show that coastal wetlands are an important component of the LOAC system because unlike estuaries and inland waters, contributes an additional 10% ( $-16.9 \pm 10.4 \text{ TgC yr}^{-1}$ ) of the biospheric sink. However, we



note that the net ecosystem exchange estimated for coastal wetlands (mangroves, tidal marshes, and seagrass meadows) is based on data obtained outside Australasia because no eddy covariance data are available for the Australasia region, which makes coastal ecosystems estimates highly uncertain.

Australia's gross fire emissions constitute a large CO<sub>2</sub> flux component in the budget. For extreme fire years, such as the catastrophic and unprecedented Australia fires in 2019 when gross emissions reached  $212.8 \pm 46.3$  TgC yr<sup>-1</sup>, fire emissions are a dominant gross flux to the atmosphere. Gross fire emissions across Australia are compensated in large part by the rapid regrowth of the herbaceous components (in sparsely vegetation and savanna) that dominate Australia's landscapes, for which net fire fluxes are considered neutral on a 1–3-year timeframe. In addition, strong post-fire regrowth capacity of the southern and south-eastern forests also offsets a dominant portion of forest fire emissions (Qin et al., 2022). Because of these vegetation responses to fire, the overall net impact of fire was  $9.9 \pm 6.2$  TgC yr<sup>-1</sup> for the decade 2010–2019, originating in the temperate and tropical savanna regions for which the net balance is provided. We note that in the carbon budget presented here, 2019 had the largest forest burned area of the past 90 years (Canadell, Costa, et al., 2021; Canadell, Meyer, et al., 2021), so any follow-up regrowth from the extensive burned area falls outside the budget period ending in December 2019.

Another important anthropogenic CO<sub>2</sub> flux affecting the net carbon balance is changes in the land use (LUC) and land management. For the decade 2010–2019, the impact of LUC on Australian fluxes was obtained from the NGHGI. We have not used data from the globally harmonized land use change database (LUH2) because it shows poorly constrained land-use transitions over Australia (i.e., classification of secondary clearing of regrown forest, or expansion of forest in protected areas). Based on Australia's NGHGI, CO<sub>2</sub> emissions from land clearing (mainly forest land converted to grasslands ( $11.0 \pm 6.3$  TgC yr<sup>-1</sup>) are more than offset by CO<sub>2</sub> sinks from softwood and hardwood plantations, environmental plantings, and natural regrowth on cleared lands ( $-14.6 \pm 1.8$  TgC yr<sup>-1</sup>), together leading to a net CO<sub>2</sub> sink to the land.

New Zealand's CO<sub>2</sub> sink is driven primarily by the growth of natural and managed forests. New Zealand's temperate climate supports a very productive pine plantation forestry industry, which is reflected in the CenW simulation. Pine forests were estimated to contribute  $20.3 \pm 0.61$  (1 $\sigma$ ) TgC yr<sup>-1</sup> to New Zealand's biospheric CO<sub>2</sub> sink. New Zealand's mature native forests were also a sink in the Biome-BGCMuSo model ( $7.8 \pm 2.6$  (1 $\sigma$ ) TgC yr<sup>-1</sup>) and the CarbonWatch-NZ inversion results (Bukosa et al., 2023; Steinkamp et al., 2017). Grasslands were also a sink from a territorial atmospheric perspective, albeit smaller than forests both in absolute terms and in proportion to area ( $7.0 \pm 2.3$  TgC yr<sup>-1</sup>). However, the totality of highly managed agricultural systems (e.g., pine plantation forests and pastoral dairy farming) is C-CO<sub>2</sub> neutral. In these systems, the carbon is not sequestered in the terrestrial biosphere long-term but rather exported in the form of harvested wood products or milk and meat. The CO<sub>2</sub> is eventually returned to the atmosphere via respiration on a longer timescale and/or outside of New Zealand. Australasia's non-territorial carbon emissions, mainly those embodied in the trade of Australia's metallurgical, thermal coal, and liquefied natural gas, constitute an important component of the fossil fuel emissions burned and consumed overseas. Understanding the trade flows of non-territorial carbon will become increasingly important as countries signatories to the Paris Agreement strive to achieve net zero emissions.

#### 4.2. Territorial Net Carbon Balance of Australasia: Reconciling Bottom-Up and Top-Down Estimates

We compared the balance of Australia's and New Zealand's bottom-up carbon net budgets with multiple atmospheric CO<sub>2</sub> inversions (top-down approach) based on satellite and in situ observations. The comparison allows us to explore how consistent the estimates from these two approaches are for 2010–2019, and therefore, how robust our understanding of the net CO<sub>2</sub> balance is.

For Australia, we found relatively good agreement, albeit with large uncertainty, between the bottom-up estimate and satellite/in situ-based inversion estimates for the overlapping period 2010–2019 (Figure 9b). Australia's annual net balance fluctuated from being a net CO<sub>2</sub> sink and a net source (Figure 9b), closely associated with continental rainfall anomalies (Ahlstrom et al., 2015; Detmers et al., 2015; Haverd et al., 2016; Poulter et al., 2014; Trudinger et al., 2016). This link is highlighted during the strong 2010–2011 La Niña, when the bottom-up and GOSAT estimates show a strong CO<sub>2</sub> sink likely driven by an anomalous increase in rainfall in that period (Figure S13 in Supporting Information S1). The opposite occurs during continental scale negative rainfall anomalies such as 2018, and particularly 2019, which also had record-high temperatures that together led to unprecedented levels of CO<sub>2</sub> emissions from wildfires (Qin et al., 2022). Australia 2010–2019's net decadal

balance ( $37.3 \pm 75.8 \text{ TgC yr}^{-1}$ ) was strongly influenced by the large sources in 2018 and 2019, but that influence was largely counterbalanced by the large carbon sinks in 2010/2011 and 2016/2017.

Improved satellite retrievals, such as the one used in the latest OCO-2 model intercomparison (Byrne et al., 2023), suggest that the magnitude of Australia's sink found for the 2015–2019 period should be smaller (close to neutral) than previous estimates that rely on older satellite retrievals, and highlight the importance of using accurate and precise satellite observations for the CO<sub>2</sub> flux inversion, particularly at regional scales. We note that given the large year-to-year variability, and the relatively short period covered by OCO-2, a mean flux for a 5-year period has limited value for assessing the state of the net carbon balance of Australia as it relates to longer-term dynamics.

For New Zealand, the top-down global inversions (either GOSAT or OCO-2) showed a poor level of agreement with the bottom-up estimates (Figure 9c). Only New Zealand's national inversion flux estimate (CarbonWatch-NZ), falls within the uncertainty range of our bottom-up estimates. However, it is important to note that the New Zealand bottom-up carbon budget was built using the same biospheric model (prior information) used in the New Zealand national inversion; therefore, the inversion is not fully independent of the bottom-up budget constructed for this country. We have more confidence in the New Zealand national inversion findings than the global flux inversion because this regional inversion uses New Zealand-specific prior flux information and continuous in situ measurements that provide better temporal and spatial coverage compared with satellite observations, which have many gaps and low resolution over New Zealand. The New Zealand's inversion shows a stronger sink than either the bottom-up models or New Zealand NGHGI (Bukosa et al., 2023).

### 4.3. Future Research Directions

#### 4.3.1. Biospheric Terrestrial Models

The biospheric models used in these budgets (CABLE-POP BIOS3, Biome-BGCMuSo and CenW) provide the large biospheric fluxes (GPP, NPP, NEP) contributing to the bottom-up budget and the “prior” fluxes in the regional atmospheric inversions. That makes the models involve a critical part of the construction of the budgets, and therefore, their limitations will strongly influence the final net carbon balance. Key advancements required in these models are (a) integration of high resolution and nationally based information on LUC transition maps, which is brought in this carbon budget as an external flux from the NGHGIs, and separate from the internal processes of the biospheric models; (b) integration of a fire component able to deal with changing fire regimes covering all lands and the gross fluxes of emissions and regrowth, particularly for Australia; and (c) continuation of benchmarking against observations and, to the extent possible, to assimilate those observations in model parameterization. We acknowledge that further investigation is needed to understand model structural uncertainties, and uncertainties in model parameters and forcing. In this study, large uncertainties in GPP, NPP and NEP fluxes represent the large spread between CABLE-POP, Biome-BGCMuso output and the TRENDY DVGM global model assessed in this study.

#### 4.3.2. Land Use, Land Use Change and Forestry

The management of grazed pasture is a large component of uncertainty in New Zealand's carbon budget. Although recent improvements have been made in the Biome-BGCMuSo model to enable the explicit simulation of grazing, fertilizer application, irrigation, and other management practices (Hidy et al., 2016, 2022), it is difficult to capture the full range of management practices that are in use in New Zealand. Detailed, spatially explicit data on the management of New Zealand's pastoral agriculture sector is not publicly available. Mowing of pasture for hay also occurs throughout the country, which was not included in our simulations. More work is needed to accurately model the diversity of managed grasslands not only in New Zealand but also globally. For Australia, large uncertainties remain on the role of the extensive semi-arid region in contributing to long-term trends in carbon sequestration and the relative importance of anthropogenic and natural drivers.

#### 4.3.3. Coastal Ecosystems

Despite significant interest in the use of blue carbon (mangroves, tidal marshes, seagrass meadows, and kelp forests) as a nature-based solution, Australasia has limited information on the fluxes that would enable the construction of a full carbon budget for these types of ecosystems, including NPP, carbon burial rates, export to the ocean, and import from the land. In addition, direct tower-based CO<sub>2</sub> eddy covariance measurements (NEE)

## Acknowledgments

Yohanna Villalobos, Josep G Canadell, Ian Harman, and Peter Briggs acknowledge the support of the Australian National Environmental Science Program (NESP)—Climate Systems Hub and the assistance of resources from the National Computational Infrastructure (NCI Australia), an NCRIS enabled capability supported by the Australian Government. CSIRO's authors also acknowledge Jürgen Knauer for providing assistance to the CABLE-POP model. Sara E Mikaloff-Fletcher, Beata Bukosa, Elizabeth Keller, Timothy Hilton, Donna Giltrap, Miko Kirschbaum and Liyin Liang received funding from the Government of New Zealand under the CarbonWatch-NZ Endeavour Research Programme (#C01X1817). The New Zealand-based authors would like to acknowledge Raghav Srinivasan for improving and maintaining the New Zealand Virtual Climate Station Network (VCSN) and for making the data set available for this work. The New Zealand work is additionally supported by Strategic Science Investment Funding (SSIF) from the Ministry of Business, Innovation & Employment (MBIE) under the Measurements and modeling of carbon dioxide in the New Zealand region. The NZLAM and NZCSM Numerical Weather Prediction models used in this study were developed with the support of the SSIF through the NIWA programme "Forecasting Weather Systems." Sara Mikaloff-Fletcher and Beata Bukosa also wish to acknowledge the use of New Zealand eScience Infrastructure (NeSI) high performance computing facilities, consulting support and/or training services as part of this research. New Zealand's national facilities are provided by NeSI and funded jointly by NeSI's collaborator institutions and through the Ministry of Business, Innovation & Employment's Research Infrastructure programme. URL <https://www.nesi.org.nz>. The New Zealand Material was also produced using Met Office Software. The New Zealand-based authors also wish to acknowledge Shin-Ichiro Nakaoka and Hitoshi Mukai from the National Institute for Environmental Studies Earth System Division Center for Global Environmental Studies (NIES) for the Trans Future 5 (TF5) CO<sub>2</sub> atmospheric data management, and we deeply appreciate the generous cooperation of Toyofuji Shipping Co., and Kagoshima Senpaku Co. with the NIES Volunteer Observing Ship program. We would like to thank the captain and crew of the M/S TF5. Ronny Lauerwald acknowledges funding by the French state aid managed by the ANR under the "Investissements d'avenir" programme [ANR-16-CONV-0003\_Cland]. Judith Rosentreter acknowledges funding from the Yale Institute of Biospheric Studies, Yale University.

for coastal ecosystems are needed across Australia and New Zealand to improve what is currently a highly uncertain contribution to the net carbon balance of the Australasia region.

### 4.3.4. Atmospheric Inversions

In addition to the use of global atmospheric inversions with the latest satellite retrievals from OCO-2 and GOSAT that are continuously improving, there is an opportunity to use and further explore the capabilities of higher-resolution inversion systems developed in Australia and New Zealand. Atmospheric inversion systems down to continental and regional scales are becoming increasingly capable of monitoring and assessing the effectiveness of emission reduction established by nations to tackle climate change. For Australia and New Zealand, this requires additional ground-based CO<sub>2</sub> observations and further development of inversion frameworks that can be updated regularly (e.g., on annual basis). The integration of data from the NGHGI, regionally parameterized biospheric modeling, and atmospheric inversions can create a robust and adaptive system to track and improve the estimates and drivers of the net carbon balance of Australasia and its two contributing countries.

### 4.3.5. Ground-Based Observations

Expanding the current GHG monitoring network and other ground-based observations (e.g., eddy flux towers or soil carbon measurements) across Australia and New Zealand would be beneficial to better constrain carbon budgets for both bottom-up and top-down approaches. Ground-based remote sensing observations are also reliable sources of information and reference points to validate remote sensing products.

## 5. Conclusions

We conducted a comprehensive carbon (CO<sub>2</sub>) budget assessment for Australasia as a whole, and for Australia and New Zealand individually. We used two different approaches to estimate CO<sub>2</sub> fluxes: top-down atmospheric inversions and bottom-up methods. Since the first RECCAP study published in 2013 (Haverd et al., 2013, for Australia only), a wealth of new data and improved models have become available. These are utilized fully in this new carbon-CO<sub>2</sub> budget, including the use of satellite data from OCO-2 and GOSAT. Australasia's net bottom-up CO<sub>2</sub> balance during 2010–2019 suggests that this region was carbon-CO<sub>2</sub> neutral, with large uncertainties for some of the major biospheric natural fluxes. There is high year-to-year variability of the net CO<sub>2</sub> balance, particularly for Australia, with some years neutral, a net CO<sub>2</sub> source to the atmosphere, and others a net CO<sub>2</sub> sink to the land. This high inter-annual variability, and the climatic extremes driving this variability, have a large influence on the decadal budget and make it challenging to determine long-term trends. The continued development of biospheric modeling improved satellite-based CO<sub>2</sub> fluxes, and an increase in the density of the ground-based networks of CO<sub>2</sub> measurements over Australia and New Zealand will greatly improve flux estimates and their potential for verifying the robustness of bottom-up carbon budgets.

## Conflict of Interest

The authors declare no conflicts of interest relevant to this study.

## Data Availability Statement

CABLE-POP, Biome BGC-Muso and CenW model simulations (gridded data set), and data sets related to the figures made in the manuscript are available in a public repository (<https://doi.org/10.5281/zenodo.8432132>).

## References

- Ahlstrom, A., Raupach, M. R., Schurgers, G., Smith, B., Arneeth, A., Jung, M., et al. (2015). The dominant role of semi-arid ecosystems in the trend and variability of the land CO<sub>2</sub> sink. *Science*, *348*(6237), 895–899. <https://doi.org/10.1126/science.aaa1668>
- Andrew, R. M., & Peters, G. P. (2021). The global carbon project's fossil CO<sub>2</sub> emissions dataset (2021v34) [Dataset]. Zenodo. <https://doi.org/10.5281/ZENODO.5569235>
- Australian National Inventory Report. (2019). The Australian Government submission to the United Nations framework convention on climate change Australian National Greenhouse accounts (Vol. 1). Retrieved from <https://www.dceew.gov.au/climate-change/publications/national-greenhouse-accounts-2019/national-inventory-report-2019>
- Baisden, W. T., Beets, P., Carran, R. A., Clark, H., Ford-Robertson, J. B., Francis, G. S., et al. (2001). An assessment of the significance to New Zealand of article 3.4 activities under the Kyoto protocol: A report.

- Beringer, J., Moore, C. E., Cleverly, J., Campbell, D. I., Cleugh, H., De Kauwe, M. G., et al. (2022). Bridge to the future: Important lessons from 20 years of ecosystem observations made by the OzFlux network. *Global Change Biology*, 28(11), 3489–3514. <https://doi.org/10.1111/gcb.16141>
- Brailsford, G. W., Stephens, B. B., Gomez, A. J., Riedel, K., Mikaloff Fletcher, S. E., Nichol, S. E., & Manning, M. R. (2012). Long-term continuous atmospheric CO<sub>2</sub> measurements at Baring Head, New Zealand. *Atmospheric Measurement Techniques*, 5(12), 3109–3117. <https://doi.org/10.5194/amt-5-3109-2012>
- Bukosa, B., Mikaloff-Fletcher, Sara, B., Gordon, S., Dan, M., Stuart, K., et al. (2023). CarbonWatch-NZ: National scale inverse modelling of New Zealand's carbon balance (version RECCAP2) [Dataset]. Zenodo. <https://doi.org/10.5281/zenodo.8423899>
- Byrne, B., Baker, D. F., Basu, S., Bertolacci, M., Bowman, K. W., Carroll, D., et al. (2023). National CO<sub>2</sub> budgets (2015–2020) inferred from atmospheric CO<sub>2</sub> observations in support of the global stocktake. *Earth System Science Data*, 15(2), 963–1004. <https://doi.org/10.5194/essd-15-963-2023>
- Canadell, J. G., Costa, M. H., Cotrim da Cunha, L., Cox, P. M., Eliseev, A. V., Henson, S., et al. (2021). Global carbon and other biogeochemical cycles and feedbacks. In *Climate change 2021: The physical science basis. Contribution of working group I to the sixth assessment report of the intergovernmental panel on climate change*.
- Canadell, J. G., Meyer, C. P., Cook, G. D., Cook, G. D., Dowdy, A., Briggs, P. R., et al. (2021). Multi-decadal increase of forest burned area in Australia is linked to climate change. *Nature Communications*, 12(1), 6921. <https://doi.org/10.1038/s41467-021-27225-4>
- Chandra, N., Patra, P. K., Niwa, Y., Ito, A., Iida, Y., Goto, D., et al. (2022). Estimated regional CO<sub>2</sub> flux and uncertainty based on an ensemble of atmospheric CO<sub>2</sub> inversions. *Atmospheric Chemistry and Physics*, 22(14), 9215–9243. <https://doi.org/10.5194/acp-22-9215-2022>
- Ciais, P., Bastos, A., Chevallier, F., Lauerwald, R., Poulter, B., Canadell, J. G., et al. (2022). Definitions and methods to estimate regional land carbon fluxes for the second phase of the REgional Carbon Cycle Assessment and Processes Project (RECCAP-2). *Geoscientific Model Development*, 15(3), 1289–1316. <https://doi.org/10.5194/gmd-15-1289-2022>
- Ciais, P., Rayner, P., Chevallier, F., Bousquet, P., Logan, M., Peylin, P., & Ramonet, M. (2010). Atmospheric inversions for estimating CO<sub>2</sub> fluxes: Methods and perspectives. *Climatic Change*, 103(1–2), 69–92. <https://doi.org/10.1007/s10584-010-9909-3>
- Ciais, P., Yao, Y., Gasser, T., Baccini, A., Wang, Y., Lauerwald, R., et al. (2021). Empirical estimates of regional carbon budgets imply reduced global soil heterotrophic respiration. *National Science Review*, 8(2). <https://doi.org/10.1093/nsr/nwaa145>
- Crippa, M., Solazzo, E., Huang, G., Guizzardi, D., Koffi, E., Muntean, M., et al. (2020). High resolution temporal profiles in the emissions database for global atmospheric research. *Scientific Data*, 7(1), 121. <https://doi.org/10.1038/s41597-020-0462-2>
- Detmers, R. G., Hasekamp, O., Aben, I., Houweling, S., Van Leeuwen, T. T., Butz, A., et al. (2015). Anomalous carbon uptake in Australia as seen by GOSAT. *Geophysical Research Letters*, 42(19), 8177–8184. <https://doi.org/10.1002/2015GL065161>
- Filbee-Dexter, K., & Wernberg, T. (2020). Substantial blue carbon in overlooked Australian kelp forests. *Scientific Reports*, 10(1), 12341. <https://doi.org/10.1038/s41598-020-69258-7>
- Friedlingstein, P., O'Sullivan, M., Jones, M. W., Andrew, R. M., Hauck, J., Olsen, A., et al. (2020). Global carbon budget 2020. *Earth System Science Data*, 12(4), 3269–3340. <https://doi.org/10.5194/essd-12-3269-2020>
- Friedlingstein, P., Jones, M. W., O'Sullivan, M., Andrew, R. M., Bakker, D. C. E., Hauck, J., et al. (2022). Global carbon budget 2021. *Earth System Science Data*, 14(4), 1917–2005. <https://doi.org/10.5194/essd-14-1917-2022>
- Grassi, G., Schwingshackl, C., Gasser, T., Houghton, R. A., Sitch, S., Canadell, J. G., et al. (2023). Harmonising the land-use flux estimates of global models and national inventories for 2000–2020. *Earth System Science Data*, 15(3), 1093–1114. <https://doi.org/10.5194/essd-15-1093-2023>
- Hartmann, J., Jansen, N., Dürr, H. H., Kempe, S., & Köhler, P. (2009). Global CO<sub>2</sub>-consumption by chemical weathering: What is the contribution of highly active weathering regions? *Global and Planetary Change*, 69(4), 185–194. <https://doi.org/10.1016/j.gloplacha.2009.07.007>
- Hartmann, J., Moosdorf, N., Lauerwald, R., Hinderer, M., & West, A. J. (2014). Global chemical weathering and associated P-release—The role of lithology, temperature and soil properties. *Chemical Geology*, 363, 145–163. <https://doi.org/10.1016/j.chemgeo.2013.10.025>
- Haverd, V., Raupach, M. R., Briggs, P. R., Davis, S. J., Law, R. M., Meyer, C. P., et al. (2013). The Australian terrestrial carbon budget. *Biogeosciences*, 10(2), 851–869. <https://doi.org/10.5194/bg-10-851-2013>
- Haverd, V., Smith, B., Canadell, J. G., Cuntz, M., Mikaloff-Fletcher, S., Farquhar, G., et al. (2020). Higher than expected CO<sub>2</sub> fertilization inferred from leaf to global observations. *Global Change Biology*, 26(4), 2390–2402. <https://doi.org/10.1111/gcb.14950>
- Haverd, V., Smith, B., Nieradzik, L., Briggs, P. R., Woodgate, W., Trudinger, C. M., & Canadell, J. G. (2018). A new version of the CABLE land surface model (Subversion revision r4546), incorporating land use and land cover change, woody vegetation demography and a novel optimisation-based approach to plant coordination of electron transport and carboxylation capacity. *Geoscientific Model Development Discussions*, II, 1–33. <https://doi.org/10.5194/gmd-2017-265>
- Haverd, V., Smith, B., & Trudinger, C. (2016). Process contributions of Australian ecosystems to interannual variations in the carbon cycle. *Environmental Research Letters*, 11(5), 054013. <https://doi.org/10.1088/1748-9326/11/5/054013>
- Hidy, D., Barcza, Z., Hollós, R., Dobor, L., Ács, T., Zacháry, D., et al. (2022). Soil-related developments of the Biome-BGCMuSo v6.2 terrestrial ecosystem model. *Geoscientific Model Development*, 15(5), 2157–2181. <https://doi.org/10.5194/gmd-15-2157-2022>
- Hidy, D., Barcza, Z., Marjanović, H., Ostrogović Sever, M. Z., Dobor, L., Gelybó, G., et al. (2016). Terrestrial ecosystem process model Biome-BGCMuSo v4.0: Summary of improvements and new modeling possibilities. *Geoscientific Model Development*, 9(12), 4405–4437. <https://doi.org/10.5194/gmd-9-4405-2016>
- Hunt, J. E., Laubach, J., Barthel, M., Fraser, A., & Phillips, R. L. (2016). Carbon budgets for an irrigated intensively grazed dairy pasture and an unirrigated winter-grazed pasture. *Biogeosciences*, 13(10), 2927–2944. <https://doi.org/10.5194/bg-13-2927-2016>
- Kirschbaum, M. U. F. (1999). CenW, a forest growth model with linked carbon, energy, nutrient and water cycles. *Ecological Modelling*, 118(1), 17–59. [https://doi.org/10.1016/S0304-3800\(99\)00020-4](https://doi.org/10.1016/S0304-3800(99)00020-4)
- Laruelle, G. G., Landschützer, P., Gruber, N., Ti, J. L., Delille, B., & Regnier, P. (2017). Global high-resolution monthly pCO<sub>2</sub> climatology for the coastal ocean derived from neural network interpolation. *Biogeosciences*, 14(19), 4545–4561. <https://doi.org/10.5194/bg-14-4545-2017>
- Lauerwald, R., Allen, G. H., Deemer, B. R., Liu, S., Maavara, T., Raymond, P., et al. (2023). Inland water greenhouse gas budgets for RECCAP2: 2. Regionalization and homogenization of estimates. *Global Biogeochemical Cycles*, 37(5), 1–25. <https://doi.org/10.1029/2022GB007658>
- Lowe, D. C., Guenther, P. R., & Keeling, C. D. (1979). The concentration of atmospheric carbon dioxide at Baring Head, New Zealand. *Tellus*, 31(1), 58–67. <https://doi.org/10.1111/j.2153-3490.1979.tb00882.x>
- Maavara, T., Lauerwald, R., Regnier, P., & Van Cappellen, P. (2017). Global perturbation of organic carbon cycling by river damming. *Nature Communications*, 8, 1–10. <https://doi.org/10.1038/ncomms15347>
- Matthews, H. D., Tokarska, K. B., Nicholls, Z. R. J., Rogelj, J., Canadell, J. G., Friedlingstein, P., et al. (2020). Opportunities and challenges in using remaining carbon budgets to guide climate policy. *Nature Geoscience*, 13(12), 769–779. <https://doi.org/10.1038/s41561-020-00663-3>



- Mayorga, E., Seitzinger, S. P., Harrison, J. A., Dumont, E., Beusen, A. H. W., Bouwman, A. F., et al. (2010). Global nutrient export from Watersheds 2 (NEWS 2): Model development and implementation. *Environmental Modelling & Software*, *25*(7), 837–853. <https://doi.org/10.1016/j.envsoft.2010.01.007>
- Metz, E.-M., Vardag, S. N., Basu, S., Jung, M., Ahrens, B., El-Madany, T., et al. (2023). Soil respiration-driven CO<sub>2</sub> pulses dominate Australia's flux variability. *Science*, *379*(6639), 1332–1335. <https://doi.org/10.1126/science.add7833>
- New Zealand Ministry for the Environment. (2021). New Zealand's Greenhouse gas inventory 1990–2019.
- NIWA. (2023). Overview of New Zealand's climate. Retrieved from <https://niwa.co.nz/education-and-training/schools/resources/climate/overview>
- Oda, T., Maksyutov, S., & Andres, R. J. (2018). The open-source data inventory for anthropogenic CO<sub>2</sub>, version 2016 (ODIAC2016): A global monthly fossil fuel CO<sub>2</sub> gridded emissions data product for tracer transport simulations and surface flux inversions. *Earth System Science Data*, *10*(1), 87–107. <https://doi.org/10.5194/essd-10-87-2018>
- Peiro, H., Crowell, S., Schuh, A., Baker, D. F., O'Dell, C., Jacobson, A. R., et al. (2022). Four years of global carbon cycle observed from the Orbiting Carbon Observatory 2 (OCO-2) version 9 and in situ data and comparison to OCO-2 version 7. *Atmospheric Chemistry and Physics*, *22*(2), 1097–1130. <https://doi.org/10.5194/acp-22-1097-2022>
- Peters, G. P., Davis, S. J., & Andrew, R. (2012). A synthesis of carbon in international trade. *Biogeosciences*, *9*(8), 3247–3276. <https://doi.org/10.5194/bg-9-3247-2012>
- Poulter, B., Bastos, A., Canadell, J., Ciais, P., Gruber, N., Hauck, J., et al. (2022). Inventorying Earth's land and ocean greenhouse gases. *Eos*, *103*. <https://doi.org/10.1029/2022eol179084>
- Poulter, B., Frank, D., Ciais, P., Myneni, R. B., Andela, N., Bi, J., et al. (2014). Contribution of semi-arid ecosystems to interannual variability of the global carbon cycle. *Nature*, *509*(7502), 600–603. <https://doi.org/10.1038/nature13376>
- Qin, Y., Xiao, X., Wigner, J. P., Ciais, P., Canadell, J. G., Brandt, M., et al. (2022). Large loss and rapid recovery of vegetation cover and aboveground biomass over forest areas in Australia during 2019–2020. *Remote Sensing of Environment*, *278*, 113087. <https://doi.org/10.1016/j.rse.2022.113087>
- Rayner, P. (2020). Data assimilation using an ensemble of models: A hierarchical approach. *Atmospheric Chemistry and Physics*, *20*(6), 3725–3737. <https://doi.org/10.5194/acp-20-3725-2020>
- Resplandy, L., Allison, H., Werner Bange, H., Bianchi, D., Weber, T. S., Cai, W. J., et al. (2023). A synthesis of global coastal ocean greenhouse gas fluxes. *ESS Open Archive*, April, 18. <https://doi.org/10.22541/essoar.168182303.39621839/v1>
- Rosentreter, J. A., Laruelle, G. G., Bange, H. W., Bianchi, T. S., Busecke, J. J. M., Cai, W. J., et al. (2023). Coastal vegetation and estuaries collectively reduce global warming. <https://doi.org/10.1038/s41558-023-01682-9>
- Roxburgh, S. H., Barrett, D. J., Berry, S. L., Cartel, J. O., Davies, I. D., Gifford, R. M., et al. (2004). A critical overview of model estimates of net primary productivity for the Australian continent. *Functional Plant Biology*, *31*(11), 1043–1059. <https://doi.org/10.1071/FP04100>
- Serrano, O., Lovelock, C. E., Atwood, B., Macreadie, P. I., Canto, R., Phinn, S., et al. (2019). Australian vegetated coastal ecosystems as global hotspots for climate change mitigation. *Nature Communications*, *10*(1), 1–10. <https://doi.org/10.1038/s41467-019-12176-8>
- Steinkamp, K., Mikaloff Fletcher, S. E., Brailsford, G., Smale, D., Moore, S., Keller, E. D., et al. (2017). Atmospheric CO<sub>2</sub> observations and models suggest strong carbon uptake by forests in New Zealand. *Atmospheric Chemistry and Physics*, *17*(1), 47–76. <https://doi.org/10.5194/acp-17-47-2017>
- Stephens, B. B., Brailsford, G. W., Gomez, A. J., Riedel, K., Mikaloff Fletcher, S. E., Nichol, S., & Manning, M. (2013). Analysis of a 39-year continuous atmospheric CO<sub>2</sub> record from Baring Head, New Zealand. *Biogeosciences*, *10*(4), 2683–2697. <https://doi.org/10.5194/bg-10-2683-2013>
- Stephens, B. B., Miles, N. L., Richardson, S. J., Watt, A. S., & Davis, K. J. (2011). Atmospheric CO<sub>2</sub> monitoring with single-cell NDIR-based analyzers. *Atmospheric Measurement Techniques*, *4*(12), 2737–2748. <https://doi.org/10.5194/amt-4-2737-2011>
- Tate, K. R., Scott, N. A., Parshotam, A., Brown, L., Wilde, R. H., Giltrap, D. J., et al. (2000). A multi-scale analysis of a terrestrial carbon budget in New Zealand: a source or sink of carbon? *Agriculture, Ecosystems & Environment*, *82*(1–3), 229–246. [https://doi.org/10.1016/S0167-8809\(00\)00228-0](https://doi.org/10.1016/S0167-8809(00)00228-0)
- Teckentrup, L., De Kauwe, M. G., Pitman, A. J., Goll, D. S., Haverd, V., Jain, A. K., et al. (2021). Assessing the representation of the Australian carbon cycle in global vegetation models. *Biogeosciences*, *18*(20), 5639–5668. <https://doi.org/10.5194/bg-18-5639-2021>
- Trotter, C. M., Tate, K. R., Brown, L. J., Scott, N. A., Wilde, R. H., Townsend, J. A., et al. (2004). A multi-scale analysis of a national terrestrial carbon budget and the effects of land-use change. In *Global environmental change in the ocean and lands* (pp. 311–341). TERRAPUB.
- Trudinger, C. M., Haverd, V., Briggs, P. R., & Canadell, J. G. (2016). Interannual variability in Australia's terrestrial carbon cycle constrained by multiple observation types. *Biogeosciences*, *13*(23), 6363–6383. <https://doi.org/10.5194/bg-13-6363-2016>
- van der Werf, G. R., Randerson, J. T., Giglio, L., van Leeuwen, T. T., Chen, Y., Rogers, B. M., et al. (2017). Global fire emissions estimates during 1997–2016. *Earth System Science Data*, *9*(2), 697–720. <https://doi.org/10.5194/essd-9-697-2017>
- Villalobos, Y., Rayner, P., Thomas, S., & Silver, J. (2020). The potential of Orbiting Carbon Observatory-2 data to reduce the uncertainties in CO<sub>2</sub> surface fluxes over Australia using a variational assimilation scheme. *Atmospheric Chemistry and Physics*, *20*(14), 8473–8500. <https://doi.org/10.5194/acp-20-8473-2020>
- Villalobos, Y., Rayner, P. J., Silver, J. D., Thomas, S., Haverd, V., Knauer, J., et al. (2022). Interannual variability in the Australian carbon cycle over 2015–2019, based on assimilation of Orbiting Carbon Observatory-2 (OCO-2) satellite data. *Atmospheric Chemistry and Physics*, *22*(13), 8897–8934. <https://doi.org/10.5194/acp-22-8897-2022>
- Walker, A. P., De Kauwe, M. G., Bastos, A., Belmecheri, S., Georgiou, K., Keeling, R. F., et al. (2021). Integrating the evidence for a terrestrial carbon sink caused by increasing atmospheric CO<sub>2</sub>. *New Phytologist*, *229*(5), 2413–2445. <https://doi.org/10.1111/nph.16866>
- Wall, A. M., Campbell, D. I., Mudge, P. L., Rutledge, S., & Schipper, L. A. (2019). Carbon budget of an intensively grazed temperate grassland with large quantities of imported supplemental feed. *Agriculture, Ecosystems & Environment*, *281*(April), 1–15. <https://doi.org/10.1016/j.agee.2019.04.019>
- Wang, Y. P., & Barrett, D. J. (2003). Estimating regional terrestrial carbon fluxes for the Australian continent using a multiple-constraint approach: I. Using remotely sensed data and ecological observations of net primary production. *Tellus B: Chemical and Physical Meteorology*, *55*(2), 270. <https://doi.org/10.3402/tellusb.v55i2.16706>



## References From the Supporting Information

- Allen, G. H., & Pavelsky, T. (2018). Global extent of rivers and streams. *Science*, *361*(6402), 585–588. <https://doi.org/10.1126/science.aat063>
- Chau, T. T. T., Gehlen, M., & Chevallier, F. (2022). A seamless ensemble-based reconstruction of surface ocean pCO<sub>2</sub> and air-sea CO<sub>2</sub> fluxes over the global coastal and open oceans. *Biogeosciences*, *19*(4), 1087–1109. <https://doi.org/10.5194/bg-19-1087-2022>
- Ciais, P., Borges, A. V., Abril, G., Meybeck, M., Folberth, G., Hauglustaine, D., & Janssens, I. A. (2008). The impact of lateral carbon fluxes on the European carbon balance. *Biogeosciences*, *5*(5), 1259–1271. <https://doi.org/10.5194/bg-5-1259-2008>
- Cichota, R., Snow, V. O., & Tait, A. B. (2008). A functional evaluation of virtual climate station rainfall data. *New Zealand Journal of Agricultural Research*, *51*(3), 317–329. <https://doi.org/10.1080/00288230809510463>
- Crippa, M., Oreggioni, G., Guizzardi, D., Muntean, M., Schaaf, E., Lo Vullo, E., et al. (2019). JRC Science for Policy Report Fossil CO<sub>2</sub> & GHG emissions of all world countries. <https://doi.org/10.2760/687800>
- Darmenov, A., & da Silva, A. M. (2015). The quick fire emissions dataset (QFED)—Documentation of versions 2.1, 2.2 and 2.4. In *NASA technical report series on global modeling and data assimilation* (Vol. 32).
- Davies, T., Cullen, M. J. P., Malcolm, A. J., Mawson, M. H., Staniforth, A., White, A. A., & Wood, N. (2005). A new dynamical core of the Met Office's global and regional modelling of the atmosphere. *Quarterly Journal of the Royal Meteorological Society*, *131*(608), 1759–1782. <https://doi.org/10.1256/qj.04.101>
- Di Giuseppe, F., Rémy, S., Pappenberger, F., & Wetterhall, F. (2017). Combining fire radiative power observations with the fire weather index improves the estimation of fire emissions. *Atmospheric Chemistry and Physics Discussions*, 1–16. <https://doi.org/10.5194/acp-2017-790>
- Doherty, J. (2015). *Calibration and uncertainty analysis for complex environmental models*. Watermark Numerical Computing. ISBN: 978-0-9943786-0-6.
- Dürr, H. H., Laruelle, G. G., van Kempen, C. M., Slomp, C. P., Meybeck, M., & Middelkoop, H. (2011). Worldwide typology of nearshore coastal systems: Defining the estuarine filter of river inputs to the oceans. *Estuaries and Coasts*, *34*(3), 441–458. <https://doi.org/10.1007/s12237-011-9381-y>
- Faostat (2022). Food and agriculture data from food and agriculture organization (FAO) of the United Nations. Retrieved from <https://www.fao.org/faostat/en/#data>
- Grant, I., Jones, D., Wang, W., Fawcett, R., & Barratt, D. (2008). Meteorological and remotely sensed datasets for hydrological modelling: A contribution to the Australian water Availability project. In *Proceedings of the catchment-scale hydrological modelling & data assimilation (CAHMDA-3) international workshop on hydrological prediction: Modelling, observation and data assimilation*. Retrieved from <http://www.bom.gov.au/climate/austmaps/metadata-daily-solar-exposure.shtml>
- Jenkinson, D. S., Adams, D. E., & Wild, A. (1991). Model estimates of CO<sub>2</sub> emissions from soil in response to global warming. *Nature*, *351*(6324), 304–306. <https://doi.org/10.1038/351304a0>
- Jones, A., Thomson, D., Hort, M., & Devenish, B. (2007). The U.K. Met Office's next-generation atmospheric dispersion model, NAME III. In *Air pollution modeling and its application XVII* (pp. 580–589). Springer US. [https://doi.org/10.1007/978-0-387-68854-1\\_62](https://doi.org/10.1007/978-0-387-68854-1_62)
- Jones, D., Wang, W., & Fawcett, R. (2009). High-quality spatial climate data-sets for Australia. *Australian Meteorological and Oceanographic Journal*, *58*(Issue 04), 233–248. <https://doi.org/10.22499/2.5804.003>
- Kaiser, J. W., Heil, A., Andreae, M. O., Benedetti, A., Chubarova, N., Jones, L., et al. (2012). Biomass burning emissions estimated with a global fire assimilation system based on observed fire radiative power. *Biogeosciences*, *9*(1), 527–554. <https://doi.org/10.5194/bg-9-527-2012>
- Keller, E. D., Baisden, W. T., Timar, L., Mullan, B., & Clark, A. (2014). Grassland production under global change scenarios for New Zealand pastoral agriculture. *Geoscientific Model Development*, *7*(5), 2359–2391. <https://doi.org/10.5194/gmd-7-2359-2014>
- Kirschbaum, M. U. F., Guo, L. B., & Gifford, R. M. (2008). Observed and modelled soil carbon and nitrogen changes after planting a Pinus radiata stand onto former pasture. *Soil Biology and Biochemistry*, *40*(1), 247–257. <https://doi.org/10.1016/j.soilbio.2007.08.021>
- Kirschbaum, M. U. F., Watt, M. S., Tait, A., & Ausseil, A. G. E. (2012). Future wood productivity of Pinus radiata in New Zealand under expected climatic changes. *Global Change Biology*, *18*(4), 1342–1356. <https://doi.org/10.1111/j.1365-2486.2011.02625.x>
- Krausmann, F., Erb, K. H., Gingrich, S., Lauk, C., & Haberl, H. (2008). Global patterns of socioeconomic biomass flows in the year 2000: A comprehensive assessment of supply, consumption and constraints. *Ecological Economics*, *65*(3), 471–487. <https://doi.org/10.1016/j.ecolecon.2007.07.012>
- Landcare Research. (2010). Fundamental soil layer—New Zealand soil classification [Dataset]. Landcare Research. Retrieved from <https://soils.landcareresearch.co.nz/tools/fsl/>
- Landcare Research. (2020). LCDB v5.0—Land cover database version 5.0, Mainland, New Zealand [Dataset]. Landcare Research. <https://doi.org/10.26060/W5B4-WK93>
- Landschützer, P., Gruber, N., & Bakker, D. C. E. (2016). Decadal variations and trends of the global ocean carbon sink. *Global Biogeochemical Cycles*, *30*(10), 1396–1417. <https://doi.org/10.1002/2015GB005359>
- Landschützer, P., Gruber, N., & Bakker, D. C. E. (2020a). *An observation-based global monthly gridded sea surface pCO<sub>2</sub> product from 1982 onward and its monthly climatology (NCEI accession 0160558) version 5.5*. NOAA National Centers for Environmental Information. <https://doi.org/10.7289/V5Z899N6>
- Landschützer, P., Laruelle, G. G., Roobaert, A., & Regnier, P. (2020b). A uniform pCO<sub>2</sub> climatology combining open and coastal oceans. *Earth System Science Data*, *12*(4), 2537–2553. <https://doi.org/10.5194/essd-12-2537-2020>
- Laruelle, G. G., Rosentreter, J. A., & Regnier, P. (2023). Extrapolation based regionalized re-evaluation of the global estuarine surface area. *Preprint at Earth*. ArXiv doi. <https://doi.org/10.31223/X5X664>
- Maa vara, T., Lauerwald, R., Laruelle, G. G., Akbarzadeh, Z., Bouskill, N. J., Van Cappellen, P., & Regnier, P. (2019). Nitrous oxide emissions from inland waters: Are IPCC estimates too high? *Global Change Biology*, *25*(2), 473–488. <https://doi.org/10.1111/gcb.14504>
- Mandersson, A., Hoogendoorn, C., & Newsome, P. (2019). *Grassland improvement mapping using innovative data analysis (IDA) techniques—Manaaki Whenua Landcare research*. New Zealand Contract Report. LC3373.
- McKenzie, N., Jacquier, D. W., Ashton, L. J., & Cresswell, H. P. (2000). Estimation of soil properties using the Atlas of Australian Soils. CSIRO land and water technical report 11/00 (Issue February).
- McKenzie, N., & Johh, H. (1992). Interpretations of the Atlas of Australian soils. In *Consulting report to the environmental resources information network (ERIN). CSIRO division of soils technical report 94/1992*.
- Mendonça, R., Müller, R. A., Clow, D., Verpoorter, C., Raymond, P., Tranvik, L. J., & Sobek, S. (2017). Organic carbon burial in global lakes and reservoirs. *Nature Communications*, *8*(1), 1694. <https://doi.org/10.1038/s41467-017-01789-6>
- Messenger, M. L., Lehner, B., Grill, G., Nedeva, I., & Schmitt, O. (2016). Estimating the volume and age of water stored in global lakes using a geo-statistical approach. *Nature Communications*, *7*, 1–11. <https://doi.org/10.1038/ncomms13603>

- Ministry for Primary Industries. (2021). Ministry for primary industries 2021. National exotic forest description as at 1 April 2021. Retrieved from <https://www.mpi.govt.nz/>
- Müller, A., Tanimoto, H., Sugita, T., MacHida, T., Nakaoka, S. I., Patra, P. K., et al. (2021). New approach to evaluate satellite-derived XCO<sub>2</sub> over oceans by integrating ship and aircraft observations. *Atmospheric Chemistry and Physics*, 21(10), 8255–8271. <https://doi.org/10.5194/acp-21-8255-2021>
- New Zealand Ministry for the Environment. (2020). Measuring emissions: A guide for organisations: 2020 detailed guide.
- New Zealand Ministry for the Environment. (2016). New Zealand ministry for the environment: LUCAS NZ land use map (v008) [Dataset]. New Zealand Ministry for the Environment. Retrieved from <https://data.mfe.govt.nz/layer/52375-lucas-nz-land-use-map-1990-2008-2012-2016-v011/>
- Pingoud, K., Skog, K. E., Martino, D. L., Mario, T., & Xiaoqun, Z. (2006). Chapter 12: Harvested wood products. Volume 4, agriculture, forestry, and other land use (AFOLU). In *2006 IPCC guidelines for national greenhouse gas inventories* (Vol. 1–33).
- Rayner, P., Michalak, A. M., & Chevallier, F. (2016). Fundamentals of data assimilation. *Geoscientific Model Development Discussions*, 1–21. <https://doi.org/10.5194/gmd-2016-148>
- Regnier, P., Resplandy, L., Najjar, R. G., & Ciais, P. (2022). The land-to-ocean loops of the global carbon cycle. *Nature*, 603(7901), 401–410. <https://doi.org/10.1038/s41586-021-04339-9>
- Richards, G., & Evans, D. M. (2000a). *Carbon accounting model for forests (CAMFor v3.35) user manual, national carbon accounting system technical report No. 26*. Australian Greenhouse Office.
- Richards, G. P., & Evans, D. (2000b). *CAMAg national carbon accounting system*. Australian Greenhouse Office.
- Rödenbeck, C., Devries, T., Hauck, J., Le Quére, C., & Keeling, R. F. (2022). Data-based estimates of interannual sea-Air CO<sub>2</sub> flux variations 1957–2020 and their relation to environmental drivers. *Biogeosciences*, 19(10), 2627–2652. <https://doi.org/10.5194/bg-19-2627-2022>
- Roobaert, A., Laruelle, G. G., Landschützer, P., Gruber, N., Chou, L., & Regnier, P. (2019). The spatiotemporal dynamics of the sources and sinks of CO<sub>2</sub> in the global coastal ocean. *Global Biogeochemical Cycles*, 33(12), 1693–1714. <https://doi.org/10.1029/2019GB006239>
- Roxburgh, S. H., Karunaratne, S. B., Paul, K. I., Lucas, R. M., Armston, J. D., & Sun, J. (2019). A revised above-ground maximum biomass layer for the Australian continent. *Forest Ecology and Management*, 432, 264–275. <https://doi.org/10.1016/j.foreco.2018.09.011>
- Running, S. W., & Coughlan, J. C. (1988). A general model of forest ecosystem processes for regional applications I. Hydrologic balance, canopy gas exchange and primary production processes. *Ecological Modelling*, 42(2), 125–154. [https://doi.org/10.1016/0304-3800\(88\)90112-3](https://doi.org/10.1016/0304-3800(88)90112-3)
- Running, S. W., & Coughland, J. C. (1991). FOREST-BGC, A general model of forest ecosystem processes for regional applications. II. Dynamic carbon allocation and nitrogen budgets. *Tree Physiology*, 9(1–2), 147–160. <https://doi.org/10.1093/treephys/9.1-2.147>
- Russell-Smith, J., Yates, C. P., Whitehead, P. J., Smith, R., Craig, R., Allan, G. E., et al. (2007). Bushfires “down under”: Patterns and implications of contemporary Australian landscape burning. *International Journal of Wildland Fire*, 16(4), 361–377. <https://doi.org/10.1071/WF07018>
- Tait (2008). Future projections of growing degree days and frost in New Zealand and some implications for grape growing. *Weather and Climate*, 28, 17. <https://doi.org/10.2307/26169696>
- Tait, A., Henderson, R., Turner, R., & Zheng, X. (2006). Thin plate smoothing spline interpolation of daily rainfall for New Zealand using a climatological rainfall surface. *International Journal of Climatology*, 26(14), 2097–2115. <https://doi.org/10.1002/joc.1350>
- Tait, A., Sturman, J., & Clark, M. (2012). An assessment of the accuracy of interpolated daily rainfall for New Zealand. *Journal of Hydrology (New Zealand)*, 25–44. Retrieve from <http://www.jstor.org/stable/43944886>
- Tait, & Liley (2009). Interpolation of daily solar radiation for New Zealand using a satellite data-derived cloud cover surface. *Weather and Climate*, 29, 70. <https://doi.org/10.2307/26169706>
- Thornton, P., Law, B., Gholz, H. L., Clark, K. L., Falge, E., Ellsworth, D., et al. (2002). Modeling and measuring the effects of disturbance history and climate on carbon and water budgets in evergreen needleleaf forests. *Agricultural and Forest Meteorology*, 113(1–4), 185–222. [https://doi.org/10.1016/S0168-1923\(02\)00108-9](https://doi.org/10.1016/S0168-1923(02)00108-9)
- Thornton, P. E., Running, S. W., & Hunt, E. (2005). Biome-BGC: Terrestrial ecosystem process model, version 4.2 [code]. <https://doi.org/10.3334/ORNLDAC/805>
- Vörösmarty, C. J., Fekete, B. M., Meybeck, M., & Lammers, R. B. (2000). Geomorphometric attributes of the global system of rivers at 30-minute spatial resolution. *Journal of Hydrology*, 237(1–2), 17–39. [https://doi.org/10.1016/S0022-1694\(00\)00282-1](https://doi.org/10.1016/S0022-1694(00)00282-1)
- Wang, Y. P., Law, R. M., & Pak, B. (2010). A global model of carbon, nitrogen and phosphorus cycles for the terrestrial biosphere. *Biogeosciences*, 7(7), 2261–2282. <https://doi.org/10.5194/bg-7-2261-2010>
- Webster, S., Uddstrom, M., Oliver, H., & Vosper, S. (2008). A high-resolution modelling case study of a severe weather event over New Zealand. *Atmospheric Science Letters*, 9(3), 119–128. <https://doi.org/10.1002/asl.172>
- Xu, X., Sharma, P., Shu, S., Lin, T. S., Ciais, P., Tubiello, F. N., et al. (2021). Global greenhouse gas emissions from animal-based foods are twice those of plant-based foods. *Nature Food*, 2(9), 724–732. <https://doi.org/10.1038/s43016-021-00358-x>
- Yamagishi, H., Tohjima, Y., Mukai, H., Nojiri, Y., Miyazaki, C., & Katsumata, K. (2012). Observation of atmospheric oxygen/nitrogen ratio aboard a cargo ship using gas chromatography/thermal conductivity detector. *Journal of Geophysical Research*, 117(4), 1–14. <https://doi.org/10.1029/2011JD016939>
- Rayner, P. J., Michalak, A. M., & Chevallier, F. (2019). Fundamentals of data assimilation applied to biogeochemistry. *Atmospheric Chemistry and Physics*, 19(22), 13911–13932. <https://doi.org/10.5194/acp-19-13911-2019>

## Erratum

In the originally published version of this article, Figures 5 and 7 in Section 3.2 and Figure S12 in the supporting information contained errors in their Y-axis color bars. The numbers indicated in the figure legends are offset by a factor of 10. The figures have been replaced, and this may be considered the authoritative version of record.